Ice front positions for Greenland glaciers (2002–2021): a spatially extensive seasonal record and benchmark dataset for algorithm validation

Xi Lu[1, 2], Liming Jiang[1, 2], Daan Li[3], Yi Liu[1, 2], Andrew J. Sole[4], Stephen J. Livingstone[4]

[1] State Key Laboratory of Precision Geodesy, Innovation Academy for Precision Measurement Science and Technology, Chinese Academy of Sciences, Wuhan 430077, China.

[2] College of Earth and Planetary Science, University of Chinese Academy of Sciences, Beijing 100049, China.

[3] College of Urban and Environmental Sciences, Yancheng Teachers University, Yancheng 224002, China.

[4] School of Geography and Planning, University of Sheffield, Sheffield, S10 2TN, UK.

Corresponding author: Liming Jiang (jlm@whigg.ac.cn)

Abstract. Glacier terminus (ice-front) positions are key indicators of glacier dynamic variability and ice–ocean–atmosphere interactions and provide essential time-varying boundary conditions for ice-sheet modelling. High-precision, spatially extensive records are therefore critical for quantifying terminus recession, improving estimates of dynamic mass loss, and supporting the development and validation of automated front-detection algorithms. However, existing manually delineated datasets are largely restricted to marine-terminating glaciers and exhibit heterogeneous spatial coverage, temporal sampling, and delineation criteria, which limits ice-sheet-scale representativeness and propagates into consolidated and automated products that depend on them for training and evaluation. Here we present GrTPD, an independent and internally consistent dataset of Greenland glacier terminus positions, providing spatially extensive, seasonally targeted coverage across marine-, land-, lake-terminating, and peripheral glaciers. The dataset comprises 19,171 terminus delineations for 465 glaciers spanning 2002–2021, derived from multi-source satellite imagery (Landsat, Sentinel-1/2, MODIS, ENVISAT, ASTER, and ERS). Delineations were produced using standardized workflows implemented in Google Earth Engine and ArcGIS, and each record is accompanied by metadata describing acquisition date, sensor, method, glacier identifier, office name, type, vertex count and ice front length. Positional accuracy was evaluated using average minimum distance (AMD) comparisons against the integrated manually delineated TermPicks dataset and the automated AutoTerm product for overlapping glaciers. Median AMD of 54 m relative to TermPicks and 67 m relative to AutoTerm indicates high geometric fidelity and positional consistency. Across spatial aggregates and time series, GrTPD shows closer agreement with TermPicks than with AutoTerm, consistent with the greater sensitivity of automated delineations to image quality, low-contrast ice–ocean mélange conditions, and heterogeneous terminus geometries. By extending coverage beyond

删除了: Calving
删除了: outlet
删除了: Calving
带格式的: 正文, 两端对齐
设置了格式: 默认段落字体
删除了: semi-automated
删除了: type, vertex
设置了格式: 默认段落字体
删除了: over
删除了: and acquisition dates
删除了: s
设置了格式: 默认段落字体
设置了格式: 默认段落字体

marine-terminating glaciers, GrTPD enables a more comprehensive assessment of Greenland glacier terminus variability and provides a high-quality benchmark for validating and intercomparing automated delineation products. The dataset is publicly available from Zenodo https://doi.org/10.5281/zenodo.18137398 (Xi et al., 2025).

1 Introduction

Mass loss from Greenland ice sheet (GrIS) contributes significantly to global sea-level rise (Shepherd et al., 2018; Frederikse et al., 2020), with nearly half of this dynamic ice loss attributed to frontal ablation (Enderlin et al., 2014; Mouginot et al., 2019). Variations in glacier terminus position, including calving fronts at marine-terminating glaciers and frontal retreat at land- and lake-terminating glaciers, provide critical insights into glacier dynamics, ice-ocean-atmosphere interactions, and act as essential time-varying boundary conditions for ice sheet modeling (Moon and Joughin, 2008; Catania et al., 2018; Nick et al., 2013; Choi et al., 2021; Otosaka et al., 2023). Spatially extensive and high-precision records of glacier terminus positions are required to assess frontal migration, constrain frontal mass fluxes, and improve the predictive capabilities of both process-based and machine learning models (Andersen et al., 2019; Fürst et al., 2015; Kc et al., 2025; Fahrner et al., 2021; Fahrner et al., 2025).

Over the past two decades, several manually delineated datasets of glacier calving front positions derived from optical or radar satellite imagery have provided valuable insights into glacier retreat patterns and terminus variability for marine-terminating in Greenland (Table 1) (Murray et al., 2015a; Wood et al., 2021; Andersen et al., 2019). Most of these datasets were developed in the context of individual case studies or regional modelling efforts, and therefore cover only a subset of Greenland's marine-terminating glaciers, with annual or sporadic temporal sampling and varied delineation approaches (Cassotto et al., 2017; Kehrl et al., 2017; Carr et al., 2013; Fried et al., 2018; Howat and Eddy, 2017; Moon et al., 2015; Sakakibara and Sugiyama, 2019; Bevan et al., 2012). Such heterogeneity in spatial coverage, temporal resolution, and interpretation criteria limits the applicability of existing manually delineated datasets for ice-sheet-scale assessments and reduces their suitability for training and validating automated terminus detection algorithms. To improve spatial and temporal coverage, recent efforts have combined multiple manually derived sources into composite datasets (Table 1) (Greene et al., 2024; Goliber et al., 2022). For example, the TermPicks dataset (Goliber et al., 2022) integrates more than 39,000 manually delineated calving front traces contributed by multiple researchers, substantially enhancing data accessibility and enabling large-scale historical analyses. However, as noted by the authors, data coverage remains spatially uneven, with high trace density at well-studied glaciers and limited representation elsewhere. These limitations underscore the continued need for standardized and internally consistent manually curated datasets to support both fundamental research on glacier dynamics and the advancement of emerging front delineation techniques.

In recent years, the increasing availability of high-resolution satellite imagery, together with advances in computational capacity, has accelerated the development of automated calving front delineation methods. Machine learning and deep learning approaches have demonstrated strong potential for extracting glacier termini from large-scale remote sensing archives, enabling efficient and scalable monitoring of terminus variability at ice-sheet and multi-basin scales (Baumhoer et al., 2019; Cheng et al., 2021a; Zhang et al., 2023; Mohajerani et al., 2019; Loebel et al., 2024) These approaches are especially well suited to capturing nonlinear and asynchronous terminus changes that occur at the

删除了: high-accuracy…benchmark for validating and intercomparing automated delineation products. The dataset is publicly available from Zenodo (... [1]

删除了:)

设置了格式: 字体: Times New Roman, 小四, 无下划线, 字体颜色: 自动设置, 图案: 清除

带格式的: 普通(网站), 段落间距段前: 0 磅, 段后: 0 磅

删除了: front positions of marine-terminating glaciers are a key indicator of variations in glacier dynamics, ice–ocean interactions, and serve as critical boundary conditions for ice sheet models. High-precision, long-term records of calving front variability are essential for understanding glacier recession and calving processes, improving mass loss estimates, and supporting the development and validation of robust automated front-tracking algorithms. However, existing manual calving-front datasets vary in spatial and temporal coverage, limiting their ability to support the training, validation, which also was inherited by consolidated products based these and generalization of automated detection approaches. automated product trained based on this, existing datasets often exhibit limited spatial coverage, inconsistent temporal resolution, and heterogeneous delineation methods, which result in variable accuracy and insufficient detail, reducing the performance and transferability of automated calving front detection. Here, we present a spatially extensive, high-accuracy dataset providing spatially extensive, **seasonally targeted sampling**, and internally consistent delineations across multiple glacier types, include lake- and land-terminating glaciers, which are underrepresented in existing datasets but increasingly important for recent studies. of glacier calving front positions across Greenland, intended as a benchmark for algorithm training, model–data integration, and studies of seasonal glacier dynamics. The dataset comprises approximately 12xx,000 Semi-automated manually delineated calving front positions for ~290xx outlet glaciers from 2002 through 2021, extracted from multi-source satellite imagery (Landsat, Sentinel-1/2, MODIS, ENVISAT, and ERS). Delineations were conducted using standardized workflows in the Google Earth Engine platform and ArcGIS, and each record is accompanied by comprehensive metadata, including acquisition date, digitization method, source imagery, glacier type, name, and other relevant attributes. Positional accuracy was evaluated through comparison with high-resolution PlanetScope imagery and manually interpreted reference datasets, confirming high geometric fidelity with positional offsets ranging from about 40 to 100 m compared to auto products across representative glaciers, depending on ima ... [2]

删除了: s…(GrIS) contributes significantly to remains a dominant driver of contemporary …lobal sea- …evel rise (Shepherd et al., 2018; Frederikse et al., 2020), ...with For the Greenland Ice Sheet (GrIS), …early half of this dynamic ice loss is…attributed to frontal ablation at marine-terminating outlet glaciers, primarily through calving and submarine melting … ADDIN EN.CITE (Enderlin ... [3]

带格式的: 两端对齐

删除了: across …or marine-terminating in Greenland (Table 1) (Murray et al., 2015a; Wood et al., 2021; Andersen et al., 2019). However, …m…st of these datasets were developed in the context of individual case studies or regional modelling efforts, and thereforeconsequently…cover only a subset of Greenland's outlet …arine-terminating glaciers, with annual or …sporadic ... [4]

删除了: ↵
~~(Cheng et al., 2021b; Zhang et al., 2023).~~ ... [5]

individual-glacier scale (Brough et al., 2023; Catania et al., 2020; Choi et al., 2021). Despite these advantages, the performance transferability, and uncertainty characterization of automated approaches remains heavily dependent on the availability of high-quality, manually delineated training and validation data (Zhang et al., 2023). Recent studies consistently show that automated algorithms benefit from larger and more diverse training datasets that span a wide range of glacier geometries, surface conditions, temporal sampling, and sensor types (Herrmann et al., 2023; Loebel et al., 2024). For example, Cheng et al. (2021) trained deep learning models using more than 1,500 labelled calving fronts but extracted only ~22,000 Greenland termini, representing a small fraction of the available satellite scenes. By incorporating the integrated TermPicks dataset for training, Zhang et al. (2023) increased this number to 278,239, demonstrating that expanded and higher-quality training data substantially improve model generalization, while also highlighting the continued need for more extensive and diverse manual reference datasets.

More generally, deep learning models trained on regionally concentrated or glacier-type-limited datasets exhibit reduced generalizability across the full range of terminus configurations and environmental conditions present in GrIS (Zhang et al., 2023). The strong marine focus of existing manually delineated terminus datasets therefore propagates into automated glacier front detection methods. Most automated delineation algorithms, including deep learning approaches, are trained using manually curated reference data and therefore inherit similar spatial coverage and glacier-type biases, with a predominant focus on marine-terminating glaciers(Cheng et al., 2021a). This limits their ability to generalize to land-terminating and lake-terminating glaciers, which exhibit distinct terminus geometries and surface conditions. With enhanced surface melt, a growing number of previously stable land-terminating glaciers are now experiencing accelerated frontal retreat and dynamic adjustment(Fitzpatrick et al., 2013; Sundal et al., 2011; Tedstone et al., 2015), while lake-terminating glaciers show increasing spatial extent and temporal variability(Holt et al., 2024; Grimes et al., 2024). These glacier types are therefore becoming increasingly relevant for both glacier-dynamics research and ice-sheet-scale assessments(Grimes et al., 2024). Expanding manually curated training datasets to explicitly include a broader range of glacier types is thus essential, not only to supplement existing marine-terminating datasets for direct scientific analysis, but also to improve the generalization, robustness, and transferability of automated terminus delineation algorithms. While automated approaches provide powerful and scalable solutions for large-scale terminus monitoring, comprehensive and consistently curated manual datasets remain indispensable for independent validation, robust uncertainty quantification, and continued algorithm development (Moon et al., 2015; Baumhoer et al., 2019).

In response to these limitations, we present GrTPD, an independent and internally consistent dataset of glacier terminus positions for the GrIS. GrTPD provides spatially extensive and seasonally targeted sampling across marine-, land-, lake-terminating, and peripheral glaciers, addressing key gaps in existing manually delineated products. Glaciers included in GrTPD were selected primarily based on surface-flow characteristics observable in remote sensing imagery. Specifically, selected glaciers exhibit coherent surface flow features that converge toward a well-defined terminus at the ice-sheet margin, allowing reliable identification of terminus position across time. For glaciers where surface-flow features or terminus were less distinct, glacier selection was further guided by existing glacier inventories and terminus datasets, including TermPicks, AutoTerm, Bjørk et al. (2015), and NunaGIS geographic map, supporting glacier identification, naming consistency, and coverage completeness. The dataset comprises

~~(Cheng et al., 2021b; Zhang et al., 2023).~~
~~(Cheng et al., 2021b; Zhang et al., 2023).~~
~~(Cheng et al., 2021b; Zhang et al., 2023).~~
~~(Cheng et al., 2021b; Zhang et al., 2023).~~
~~(Cheng et al., 2021b; Zhang et al., 2023).~~
删除了: ~~(Cheng et al., 2021b; Zhang et al., 2023).~~
删除了: In addition
删除了: relatively small or
删除了:
删除了: often
删除了: lack sufficient generalizability
删除了: full
删除了: range
删除了:
删除了: glacier types
删除了: found
删除了: Greenland
删除了: Thus, w
删除了: —particularly deep learning methods—
删除了: calving
删除了: front
删除了: their accuracy and transferability remain limited by the scarcity of high-quality training and validation data. Until such models achieve greater robustness and generalizability, ... [6]
删除了: However, most existing calving front products suffer ... [7]
删除了: ~~The continued lack of large-scale, uniformly process~~ ... [8]
删除了: ↵ ... [9]
设置了格式: 字体: (中文) +中文正文 (宋体)
设置了格式: 字体: (中文) +中文正文 (宋体)
设置了格式: 字体: (中文) +中文正文 (宋体)
设置了格式 ... [10]
设置了格式: 字体: (中文) +中文正文 (宋体)
设置了格式: 默认段落字体
设置了格式: 删除线
设置了格式: 字体: (中文) +中文正文 (宋体)
设置了格式: 默认段落字体, 字体: (中文) +中文正文 (宋体)
设置了格式: 字体: (中文) +中文正文 (宋体)
设置了格式: 字体: (中文) +中文正文 (宋体)
设置了格式: 字体: 非加粗

19,171 terminus delineations for 465 glaciers spanning the period 2002–2021, derived from multi-source satellite imagery including Landsat, Sentinel-1/2, MODIS, ENVISAT, ASTER, and ERS. The glacier sample includes 346 marine-terminating glaciers (MT), 61 land-terminating glaciers (LT), 39 lake-terminating glaciers (LK), and 19 peripheral glaciers (PG) (Fig. 1). By extending terminus observations beyond marine-terminating glaciers, GrTPD captures a broader spectrum of terminus geometries and dynamic behaviours associated with enhanced surface melt, increasing retreat of land-terminating glaciers, and the growing prevalence of lake-terminating glaciers.

Table 1: Summary of publicly available glacier ice front datasets for the GrIS. Greene et al. (2024) provides mask-based products without glacier-specific delineations.

Production source	Glacier count	Time span	Temporal Resolution	Method
This dataset	465	2002-2021	Monthly to annual	GEEDiT, ArcGIS
Greene et al. (2024)	—	1985-2022	Monthly	Interpolated Greenland-wide mask
TermPicks (Goliber et al., 2022)	278	1916-2020	Monthly to decadal	Data compilation
AutoTerm (Zhang et al., 2023).	295	1984-2021	Monthly to decadal	Machine learning
Wood et al. (2021)	226	1992-2017	Annual	Manual
Fahrner et al. (2021)	224	1984-2017	Annual	GEEDiT
MEaSUREs(Black and Joughin, 2023)	219	2015-2021	Weekly to monthly	Manual
Murray et al. (2015b)	199	2000-2010	Annual	Manual
CALFIN(Cheng et al., 2021b)	65	1972-2019	Sub-annual	Deep learning
Andersen et al. (2019)	47	1999-2018	Annual	Manual
Loebel et al. (2024)	23	2013–2021	Seasonal	Deep learning

设置了格式: 字体: (中文) +中文正文 (宋体)

设置了格式: 字体: (默认) Times New Roman, (中文) +中文正文 (宋体)

设置了格式: 字体: (默认) Times New Roman, (中文) +中文正文 (宋体)

设置了格式: 字体: (中文) Times New Roman

下移了 [1]: Beyond its observational utility, the dataset has also been applied as a time-varying boundary condition in high-resolution transient ice flow modeling, enhancing model-data integration (Lu et al., 2025).

删除了: introduce a new dataset comprising ~12,000 manually calving front positions for ~290 outlet glaciers across GrIS from 2002 through 2021 (Fig. 1). The glaciers were chosen based on four criteria. We process all glaciers which (1) are part of the AP Ice Sheet, (2) are marine-terminating, (3) are listed in the Scientific Committee on Antarctic Research (SCAR) Composite Gazetteer of Antarctica (Cervellati et al., 2000) and (4) have a minimum calving front length of 5 km. The first three criteria define the scope of this dataset. By integrating multi-source satellite imagery and employing standardized delineation workflows, this dataset provides near-complete spatial coverage and captures both short-term fluctuations and long-term retreat trends.

删除了: By filling critical gaps in spatial completeness, temporal frequency, and methodological consistency, this product offers a robust foundation for studies of glacier dynamics and mass balance, as well as for the development and validation of automated front-tracking algorithms.

删除了: **calving**

格式化表格

删除了: ~290

删除了: Seasonal

删除了: monthly

删除了: Decadal

删除了: monthly

设置了格式: 字体: (默认) Times New Roman, (中文) Times New Roman, (中文) 中文(中国)

格式化表格

设置了格式: 字体: (默认) Times New Roman, 小四, 字体颜色: 自动设置, 图案: 清除

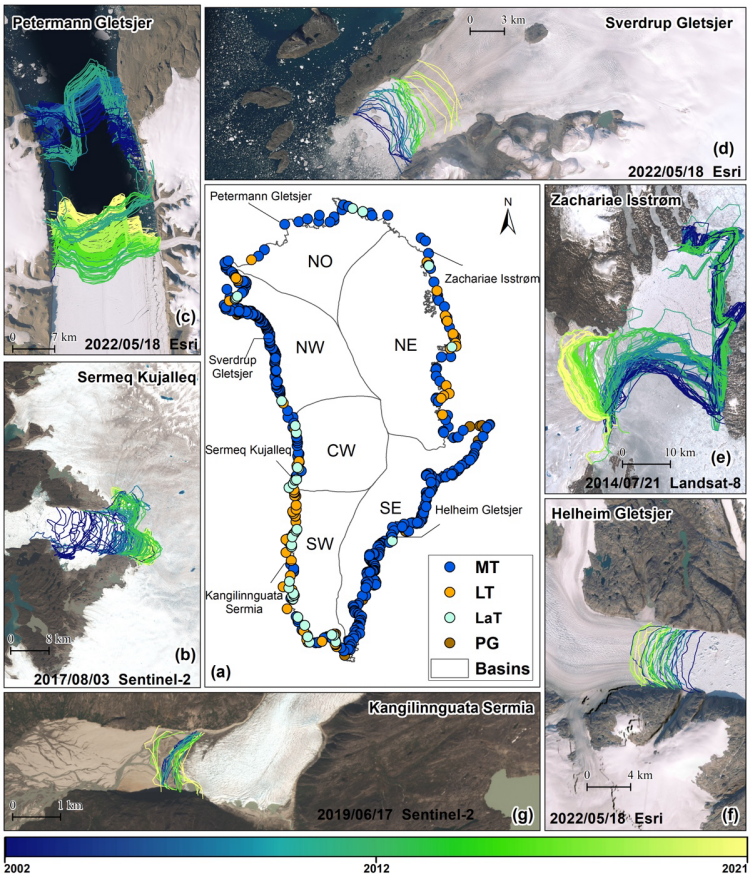

Figure 1: Spatial overview of the glaciers in Greenland included in this dataset. Central panel (a) shows glacier locations grouped by drainage basin. Surrounding maps illustrate (b–g) six examples of temporally resolved calving front positions (color-coded by year) derived from multi-source imagery.

2 Data and methodology

删除了：

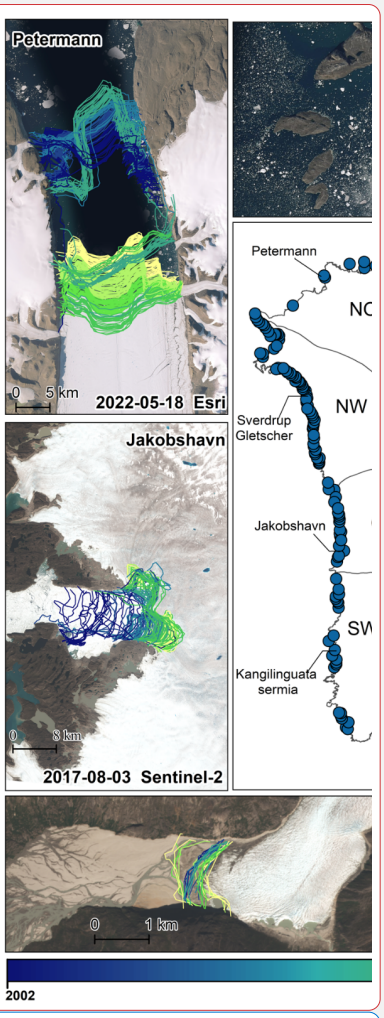

删除了：(a)

删除了：outlet …laciers in Greenland included in this dataset. Central panel (a) shows glacier locations grouped by drainage basin. Surrounding maps illustrate (b–g) some ... [11]

删除了：Sermia

删除了：2.1 Scope

2.1 Ice front delineation procedure

The delineation of glacier termini was performed through a standardized workflow integrating tool-assisted digitization and manual interpretation. The procedure comprises three primary components: (1) satellite image selection and preparation, (2) terminus delineation and geometric editing, and (3) quality control and post-processing.

To construct a spatially extensive and seasonally targeted record of glacier terminus positions across the Greenland Ice Sheet (GrIS) from 2002 to 2021, we delineated glacier termini using multi-source satellite imagery from both optical and synthetic aperture radar (SAR) sensors (Table 2). The primary data sources include optical imagery from Landsat-5, Landsat-7, Landsat-8, Sentinel-2 and ASTER, as well as SAR imagery from Sentinel-1. To improve temporal continuity and increase sampling density for selected large and dynamically important glaciers—Sermeq Kujalleq (Jakobshavn Isbræ), Petermann Gletsjer, and Zachariae Isstrøm—additional satellite imagery was incorporated outside the GEEDiT framework. These supplementary datasets include Moderate Resolution Imaging Spectroradiometer (MODIS) (Hall et al., 2002), ENVIronmental monitoring SATellite (ENVISAT) Advanced Synthetic Aperture Radar (ASAR) (Image Mode, ~8 m), and European Remote Sensing satellite (ERS-1/2) SAR (Precision Image mode, ~12.5 m) (Rignot and Kanagaratnam, 2006) were manually downloaded and processed outside of GEEDiT. The supplementary data were particularly useful during extended cloud cover or in early years of the study period where optical imagery was limited. A complete overview of all sensors, resolutions, and acquisition periods is provided in Table 2.

Table 2: Summary of satellite remote sensing imagery used for ice front position delineation.

Platform	Spatial resolution	Data level	Period used	Providers
Landsat-5	30m (multispectral)	Level-1	2006-2009	USGS
Landsat-7	30 m (multispectral)	Level-1	2002 - 2014	USGS
Landsat-8	30m (multispectral)	Level-1	2013 - 2014	USGS
MODIS	250 m (Band 1)	Level-2	2002 - 2014	USGS
Sentinel-1	10 m (IW mode)	Level-1	2014 - 2021	ESA
Sentinel-2	10 m (Bands 2-4)	Level-1C	2015- 2021	ESA
ENVISAT	~8 m (Image Mode)	Level-1B	2002-2011	ESA
ERS-1/2	12.5 m (Precision Image)	Level-1.5	2002-2011	ESA
ASTER	15m (VNIR)	Level-1T	2002–2011	NASA

删除了： Glacier terminus configurations may evolve over time, particularly for land-terminating glaciers undergoing sustained retreat and for lake-terminating glaciers that can exhibit seasonal or interannual transitions. To ensure a consistent and unambiguous classification across the dataset, glacier types are defined with respect to conditions at the **end of the observation period**, rather than varying terminus states at individual observation dates. Specifically, glacier classification is based on optical satellite imagery and supraglacial and proglacial lake inventories from **2021**, which represents the terminal epoch of the dataset. Glaciers whose termini were in direct contact with the ocean at this reference time were classified as **marine-terminating**, whereas glaciers terminating against persistent proglacial lakes were classified as **lake-** ... [12]
删除了: **2**
删除了: **Satellite imagery**
带格式的: 两端对齐, 缩进: 首行缩进: 2 字符
删除了: and
删除了: All primary datasets were accessed, visualized, and ... [13]
删除了: glacier termini across Greenland from 2002 through ... [14]
删除了: (MOD09GQ, 250 m)
删除了: ERS-1/2
删除了: European Remote Sensing satellite
删除了: These data were particularly useful during extended ... [15]
删除了: **calving**
设置了格式: 字体: 小五, 加粗
设置了格式: 字体: 加粗
带格式的: 正文
删除了: **Time range for employment**
删除了: 15 m (pan)
删除了: ?
删除了: （
删除了: ）
删除了: TP
设置了格式 ... [16]
设置了格式: 字体: (默认) 宋体, (中文) 宋体
删除了: 15
删除了: pan
删除了: TP
删除了: 15m
删除了: pan
删除了: TP
删除了: GRD
删除了: , 8
格式化表格

All primary satellite images were accessed, visualized, and digitized using the Google Earth Engine Digitisation Tool (GEEDiT) (Lea, 2018), following the standardized procedures described therein, without additional image preprocessing. To maximize data utilization and avoid unnecessary data exclusion, no fixed cloud-coverage threshold was imposed during image selection. Instead, image suitability for terminus delineation was assessed through visual inspection, based on whether the glacier terminus could be reliably identified. In ambiguous cases—such as scenes affected by dense ice mélange, shadowing, or low ice–water contrast—adjacent satellite acquisitions within a ±15-day temporal window was consulted to support cross-validation and ensure consistent interpretation of terminus position. This approach reduces the risk of misinterpretation associated with single-scene ambiguity while preserving the seasonally targeted sampling strategy.

The additional imagery was manually downloaded, georeferenced and digitized in ENVI and ArcGIS. MODIS daily imagery (Level-2 Gridded products) was used as an auxiliary dataset for three target glaciers to improve monthly temporal continuity during periods when high-resolution optical imagery was insufficient for regular terminus digitization. The surface reflectance was atmospherically corrected and georeferenced. To enhance interpretability, we computed Normalized Difference Water Index (NDWI) from red and near-infrared bands. Due to its relatively coarse spatial resolution, MODIS imagery was not used for precise terminus geometry delineation. Instead, it served as a qualitative reference to constrain the direction and magnitude of terminus change between successive high-resolution observations. Over monthly timescales, terminus migration at these glaciers is generally gradual and approximately linear, allowing MODIS-derived signals to provide supporting evidence for interpolating terminus positions between adjacent months with limited high-resolution coverage. For ENVISAT ASAR, radiometric calibration to sigma nought (dB) was applied, followed by terrain correction using the ArcticDEM digital elevation model, which provides high-resolution surface elevation coverage for the GrIS, and speckle filtering using Refined Lee filter to enhance interpretability. For ERS-1/2 precision image products, additional terrain correction and filtering were performed to ensure spatial consistency with ENVISAT. All SAR scenes were georeferenced and reprojected to a common geographic coordinate system (WGS84, EPSG:4326) for integration with optical imagery and cross-sensor comparison.

All digitized ice front positions were subsequently reviewed and, where necessary, manually adjusted to ensure spatial continuity and temporal consistency within each glacier time series. A temporal plausibility check was applied to identify unrealistic frontal advances, abrupt reversals, or anomalous migration between temporally adjacent terminus positions. Following the approach adopted in Baumhoer et al. (2019) and Zhang et al. (2023), anomalously large positional changes between the two temporally closest termini—equivalent to outliers in a terminus-change time series—were flagged for further inspection. When the overall terminus geometry remained smooth and the temporal derivative of terminus change was physically plausible, the delineation was retained. In contrast, when an anomalous migration between adjacent termini suggested a potential delineation error, the corresponding satellite imagery from the preceding and subsequent acquisition dates was retrieved for verification. If the large positional change was confirmed to reflect a calving event or terminus disintegration, the delineation was accepted; otherwise,the affected terminus trace was re-digitized. After completion of all quality-control procedures and any necessary re-editing, the validated glacier-terminus layers were packaged and distributed in GeoPackage (GPKG) format.

删除了: **2.2 3 Calving front delineation procedure**
The delineation of glacier termini was performed through a standardized workflow integrating manual interpretation and semi-automated digitization, as illustrated in Fig. 2. The procedure comprises three primary components: (1) satellite image preparation, (2) terminus extraction and editing, and (3) quality control and metadata creation and integration.
For the majority of Landsat-5, Landsat-7, Landsat-8, and Sentinel-1/2 images, calving front de

带格式的: 两端对齐

删除了: lineation was conducted directly within GEEDiT, which enables efficient visual interpretation and shapefile export without additional preprocessing (Goliber et al., 2022; Lea, 2018). For sensors not accessible via GEEDiT—including MODIS, ENVISAT ASAR, and ERS SAR—data were manually downloaded and processed externally using the ENVI and ArcGIS platform. MODIS

删除了: 09GQ

删除了: an auxiliary dataset during periods of limited optical coverage.

删除了: It is worth mentioning that MODIS, due to its low resolution, mainly serves as a reference for the calving front changes during the acquisition period of two high-resolution images, assisting in the identification of sudden calving.

删除了: ENVISAT ASAR (Level-1B) and ERS-1/2 SAR (Level-1.5) scenes were downloaded from the ESA archives.

删除了: ,

删除了: using a

删除了: DEM

删除了: (

删除了:)

设置了格式: 字体: (默认) Times New Roman, (中文) Times New Roman

删除了: were applied to

删除了:

删除了: All SAR scenes were reprojected to WGS84 (EPSG:4326) for integration with other datasets.

设置了格式: 字体: (中文) Times New Roman

删除了: Calving front positions were identified manually by visually interpreting the boundary between grounded ice and open ocean or ice mélange. Digitization was conducted at the native resoluti ... [17]

删除了: All digitized calving fronts were subsequently reviev ... [18]

设置了格式: 字体: (中文) +中文正文 (宋体), 不检查拼写或语法

设置了格式: 字体: (中文) +中文正文 (宋体), 不检查拼写或语法

设置了格式 ... [19]

设置了格式: 字体: (中文) +中文正文 (宋体), 不检查拼写或语法

设置了格式 ... [20]

设置了格式: 字体: (中文) +中文正文 (宋体), 不检查拼写或语法

删除了: . That is, the abnormally migration by the two tempo ... [21]

2.4 Attributes and metadata generation

To ensure internal consistency, interoperability, and long-term reusability, a unified attribute harmonization workflow was applied to the GrTPD dataset prior to final release. This procedure standardizes attribute content, geometry-derived metrics, and glacier-type classification across all glacier-terminus layers. For each glacier layer, attribute tables were first cleaned by removing records with missing or empty acquisition dates, ensuring that all retained geometries are temporally referenced. Only a predefined set of core attributes was preserved, while non-essential or legacy fields were removed. The retained attributes include glacier identification information, acquisition metadata, processing method, and geometric descriptors. All attribute fields were then reordered into a consistent schema to guarantee identical field structure across all glacier layers. Within each glacier layer, terminus polylines were temporally sorted by acquisition date from earliest to latest to ensure chronological consistency of the time series.

Each glacier was assigned a unique identifier (ID) formatted as "GIDxxx", aligned where possible with existing identifiers used in the TermPicks and AutoTerm datasets to facilitate cross-dataset comparison. Glaciers not covered by these reference datasets were assigned new IDs following the same numbering scheme. As a result, glacier IDs in GrTPD range from "GID001" to "GID468". In three cases, AutoTerm subdivides three single glacier terminus into two separate records; these were treated as a single glacier entity in GrTPD and assigned a single glacier ID. Glacier names (`GlacierNam`) were populated by matching glacier IDs to an external glacier-identification reference derived from Bjørk et al. (2015).

Geometric quality metrics were computed for all terminus features to ensure numerical consistency across the dataset. The number of vertices ("nvert") was recalculated directly from the polyline geometry. Terminus length ("len_km") was computed from vertex coordinates using projected distance calculations, depending on the coordinate reference system. Terminus length was defined as the cumulative piecewise length along each individual terminus trace, following the approach of (Zhang et al., 2023). All recomputed values replaced any pre-existing or inconsistent entries.

Glacier terminus type can evolve over time, particularly for land- and lake-terminating glaciers that may undergo seasonal or interannual transitions. To ensure a consistent and unambiguous classification across the dataset, glacier types were defined with respect to terminus conditions at the end of the observation period, rather than varying terminus states at individual acquisition dates. This terminal-state classification was based on optical satellite imagery and auxiliary datasets from 2021, representing the final year of the record (Joughin, 2021). Glaciers whose termini were in direct contact with the ocean at this reference time were classified as marine-terminating (MT), while glaciers terminating against persistent proglacial lakes were classified as lake-terminating (LaT). Glaciers terminating on land without sustained contact with either ocean or lake water bodies were classified as land-terminating (LT). Peripheral glaciers (PG) were identified following the classification scheme of Bjørk et al. (2015), adopting glaciers labelled as "LGIC" as the criterion for PG designation. This definition distinguishes outlet glaciers dynamically connected to the GrIS from smaller, dynamically independent glacier systems.

删除了: At
删除了: tribute harmonisation and internal consistency control
设置了格式: 字体: (中文) +中文正文 (宋体)
带格式的: 缩进: 首行缩进: 2 字符, 段落间距段前: 0 磅, 段后: 0 磅
设置了格式: 字体: (中文) +中文正文 (宋体)
设置了格式: 字体: (中文) +中文正文 (宋体)
删除了: Each calving front position was assigned a full metadata record and all ice front data were compiled into a centralized, glacier-ID-based directory structure.
设置了格式: 字体: (中文) +中文正文 (宋体), 非倾斜
设置了格式: 字体: (中文) +中文正文 (宋体)
设置了格式: 字体: (中文) +中文正文 (宋体)
设置了格式: 字体: (中文) +中文正文 (宋体)
设置了格式: 字体: (中文) +中文正文 (宋体)
设置了格式: 字体: (中文) +中文正文 (宋体)
设置了格式: 字体: (中文) +中文正文 (宋体)
设置了格式: 字体: (中文) +中文正文 (宋体)
设置了格式: 字体: (中文) +中文正文 (宋体)
设置了格式: 字体: (中文) +中文正文 (宋体)
设置了格式: 字体: (中文) +中文正文 (宋体)
设置了格式: 字体: (中文) +中文正文 (宋体)
设置了格式: 字体: (中文) +中文正文 (宋体)
设置了格式: 字体: (中文) +中文正文 (宋体)
设置了格式: 字体: (中文) +中文正文 (宋体)
设置了格式: 字体: (中文) +中文正文 (宋体)
设置了格式: 字体: (中文) +中文正文 (宋体)
设置了格式: 字体: (中文) +中文正文 (宋体)
设置了格式: 字体: (中文) +中文正文 (宋体)
设置了格式: 字体: (中文) +中文正文 (宋体)
设置了格式: 字体: (中文) +中文正文 (宋体)
删除了: (Joughin, 2021)(Joughin, 2021)
设置了格式: 字体: (中文) +中文正文 (宋体)

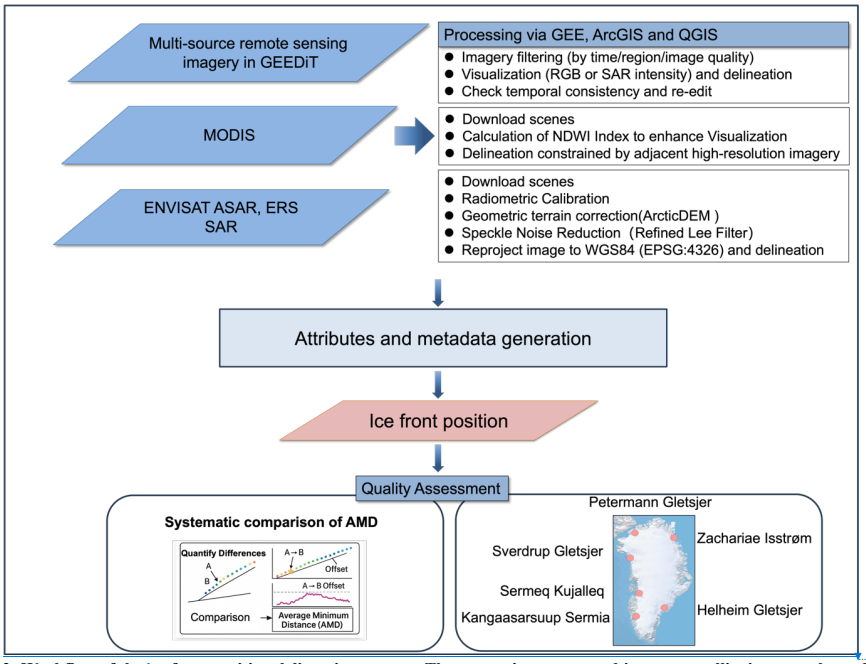

Figure 2: Workflow of the ice front position delineation process. The system integrates multi-source satellite imagery through direct access via GEE or manual preprocessing in ENVI, ArcGIS and QGIS. Glacier fronts were manually delineated, followed by quality assessment using offset metrics and cross-comparison with reference datasets.

2.3 Validation

Digitization errors of glacier ice fronts are typically on the order of the source image resolution. For instance, ice front positions derived from Landsat 7 generally exhibit planimetric uncertainties of ~25 m (Moon et al., 2015). Beyond these resolution-based limitations, manual delineation can also be affected by scene-specific factors such as low contrast, shadows, mélange cover, and interpreter subjectivity. Uncertainty quantification for automated glacier-terminus products is commonly performed by measuring the positional differences between automatically delineated termini and independently manually delineated reference traces (Cheng et al., 2021a; Zhang et al., 2023). Because machine-learning-based approaches are trained using manually delineated data, automated products generally exhibit larger positional uncertainties than manual delineations. Consequently, independently manually delineated termini are typically regarded as a reference standard for scientific analysis, model boundary constraints, and validation of automated detection methods. Several studies have evaluated the precision of manual delineation by comparing multiple independently drawn termini for the same glacier and acquisition date

删除了：To ensure internal consistency and interoperability across all glacier-terminus layers, a unified attribute harmonisation and quality-control workflow was applied to the GeoPackage dataset prior to final release. For each glacier layer, attribute tables were first cleaned by removing records with missing or empty acquisition dates, ensuring that all retained geometries are temporally referenced. Only a predefined set of core attributes was preserved, while all non-essential or legacy fields were removed. The retained attributes include glacier identification information, acquisition metadata, and geometric descriptors. Attribute fields were subsequently reordered into a consistent schema to guarantee identical field structure across all layers. All glacier-terminus polylines within each layer were then temporally sorted by acquisition date from earliest to latest. Several key attributes were either standardised or newly introduced. A unique glacier identifier (ID) was assigned based on the layer name (formatted as GID###), ensuring a one-to-one correspondence between glacier ID and layer identity. Glacier names (GlacierNam) were populated by matching glacier IDs to an external glacier identification table. A processing-method attribute (Method) was added and uniformly set to GEEDiT for all records, documenting the manual delineation approach used to generate the terminus positions.
Geometric quality metrics were recomputed for all features to ensure numerical consistency. The number of vertices (nvert) was recalculated directly from the polyline geometry, and polyline length (len_km) was recomputed from vertex coordinates using appropriate geodesic or projected distance calculations, Terminus length is determined by the sum of the piece-wise length along an individual terminus trace（zhang,2023）. depending on the coordinate reference system. These recalculated values replaced any pre-existing or inconsistent entries.
Glacier type classification (GlacierTyp) was standardised usir ... [22]

删除了：**calving**

设置了格式: 字体: (中文) Times New Roman

删除了：**and**

删除了：**2.5 Centerline construction**
For each glacier, a short centerline representing the local flow direction at the terminus was constructed in a projected coord ... [23]

删除了：calving

带格式的: 两端对齐, 缩进: 首行缩进: 2 字符

删除了：calving

设置了格式: 字体: (中文) +中文正文 (宋体)

删除了：Traditional u

设置了格式: 字体: (中文) +中文正文 (宋体)

删除了：ncertainty quantification for glacier terminus position is conducted by calculating the difference between manually picked termini and automatically-picked termini

设置了格式: 字体: (中文) +中文正文 (宋体)

设置了格式: 字体: (默认) Times New Roman, (中文) +中文正文 (宋体)

设置了格式: 字体: (默认) Times New Roman, (中文) +中文正文 (宋体)

删除了：(e.g., Cheng et al., 2020,zhang,2023). Terminus data produced from machine learning will always have larger unce ... [24]

设置了格式: 字体: (中文) +中文正文 (宋体)

(Brough et al., 2019; Fahrner et al., 2021). These repeated-drawing experiments generally yield relatively small deviations—on the order of several tens of meters—reflecting the point-by-point visual interpretation process used in manual digitization. In contrast, accuracy assessments based on comparisons among different manually delineated datasets often reveal larger discrepancies. For example, the TermPicks dataset reports a median positional difference of 107 m, with a range of 58.6 to 7,350 m, among duplicated manually traced termini, highlighting the influence of heterogeneous interpretation criteria and data sources.

To quantify the positional consistency of our glacier terminus dataset and to demonstrate its suitability as a benchmark for future algorithm development, we performed a systematic inter-product comparison against two widely used, independent terminus products: TermPicks (manual delineations) and AutoTerm (automated extractions). The comparison was designed to be robust to differences in polyline length, vertex density, and local geometric complexity, enabling objective assessment across the full set of glaciers. All terminus polylines were first harmonized to a common geographic reference system to ensure distance calculations were spatially consistent. For each glacier, records were grouped by a unique glacier identifier (GID). Terminus observations from our dataset and the comparison dataset were then matched by acquisition date. Because timestamp formats differ among products (e.g., date-only strings versus full UTC timestamps), all acquisition times were normalized to daily resolution (YYYY–MM–DD). Only dates present in both datasets for a given GID were retained. Glaciers with no overlapping acquisition dates were excluded from the statistics (but were recorded separately to document the coverage mismatch between products). We used Average Minimum Distance (AMD) as the primary quantitative metric. For each same-date pair of terminus polylines, AMD was computed as the mean of the shortest distances from points along the reference polyline to the comparison polyline (Cheng et al., 2021a).

To summaries the positional consistency between the GrTPD and existing products at both local and glacier-wide scales, we derived a set of complementary AMD-based statistics as illustrated in Fig. 3. For each glacier (identified by a unique GID), terminus polylines from the two datasets were first matched by acquisition date, retaining only same-day observations to avoid temporal aliasing. For each matched pair, point-wise average minimum distances were computed along the glacier front, yielding spatially distributed AMD profiles for each observation (Fig. 2). Detailed comparison results are provided in the Supplement. To characterize typical along-front behavior, individual AMD profiles were first interpolated onto a normalized along-front coordinate ($s/L \in [0,1]$). For each glacier, multiple profiles from different dates were then aggregated into a representative profile using the median at each s location. These glacier-level representative profiles were subsequently pooled across all glaciers, and at each normalized position the 10th, 25th, 50th, 75th, and 90th percentiles were computed, forming the quantile envelopes shown in the Fig. 3a and c. The solid median curve p50 therefore represents the typical magnitude of mismatch along the ice front, while its spread reflects spatial heterogeneity in agreement along the front. To provide a compact summary of the Fig. 3a and c distributions, we further quantified the statistics of the median curve p50(s) itself. The reported Med (p50) corresponds to the median of p50(s) over the entire front, representing a characteristic AMD level averaged along the terminus. The accompanying IQR(p50) measures the variability of this median curve along s and thus reflects along-front non-uniformity in positional agreement, rather than differences between glaciers.

删除了：For independent manually picked termini, it usually was seen a golden standard,can be direcitly used for analyse and model constraint,and used for verification of automated methods. In some studies, precision verification is also conducted, that is, multiple hand-drawn comparisons are made for the same terminal, and the differences are calculated as the uncertainty assessment result

删除了：(Fahrner et al., 2021)

删除了：(Brough et al. 2019; Fahrner et al. 2021). However, t

设置了格式: 字体: (中文) +中文正文 (宋体), (中文) 中文(中国), (其他) 英语(美国)

设置了格式: 字体: (中文) +中文正文 (宋体)

设置了格式: 字体: (中文) +中文正文 (宋体)

删除了：his magnitude is generally very small, several tens of meters,because visual interpretation and hand-drawing are carried out by drawing point by point in comparison with the remote sensing images. For accuracy verification, the differences in the repeated drawings of different manual products were compared to quantify the errors, such as Termpicks, found a median error of median error = 107 m, range = 58.6–7,350m among manually duplication traced termini

删除了：

删除了： To quantitatively evaluate the positional accuracy of the glacier terminus dataset, we performed a systematic comparison against two independent, widely used terminus products: TermPicks (manual delineations) and AutoTerm (automated extractions). The comparison was conducted using a distance-based metric desi ... [25]

设置了格式: 字体: (中文) +中文正文 (宋体)

设置了格式: 字体: (中文) +中文正文 (宋体)

设置了格式: 默认段落字体, 字体: (中文) +中文正文 (宋体)

设置了格式: 字体: (中文) +中文正文 (宋体)

设置了格式: 默认段落字体, 字体: (中文) +中文正文 (宋体)

设置了格式: 字体: (中文) +中文正文 (宋体)

设置了格式: 字体: (中文) +中文正文 (宋体)

设置了格式: 字体: (中文) +中文正文 (宋体)

设置了格式: 默认段落字体, 字体: (中文) +中文正文 (宋体)

设置了格式: 字体: (中文) +中文正文 (宋体)

设置了格式: 默认段落字体, 字体: (中文) +中文正文 (宋体)

设置了格式: 字体: (中文) +中文正文 (宋体)

设置了格式: 字体: (中文) +中文正文 (宋体)

设置了格式: 默认段落字体, 字体: (中文) +中文正文 (宋体)

设置了格式: 字体: (中文) +中文正文 (宋体)

设置了格式: 默认段落字体, 字体: (中文) +中文正文 (宋体)

设置了格式: 字体: (中文) +中文正文 (宋体)

设置了格式: 默认段落字体, 字体: (中文) +中文正文 (宋体)

设置了格式: 字体: (中文) +中文正文 (宋体)

设置了格式: 字体: (中文) +中文正文 (宋体)

设置了格式: 字体: (中文) +中文正文 (宋体)

For the along-front comparison (Fig. 3a, c), the median AMD curve p50(s) indicates a consistently lower mismatch for TermPicks relative to AutoTerm across the glacier fronts. The characteristic AMD level, summarised by Med_s (p50), is 54 m for TermPicks, compared with 67 m for AutoTerm, indicating closer overall agreement between TermPicks and the GrTPD. In addition, the spatial variability along the front, quantified by IQR_s (p50), is substantially smaller for TermPicks (11 m) than for AutoTerm (27 m), suggesting that discrepancies with the reference dataset are more spatially uniform along the ice front for TermPicks, whereas AutoTerm exhibits stronger along-front heterogeneity.

At the glacier-wide scale (Fig. 3b, d), the distribution of glacier-wise median AMD further confirms this pattern. TermPicks generally shows lower median offsets across glaciers, with reduced within-glacier variability, whereas AutoTerm displays a broader spread and higher typical mismatch values. The dashed horizontal lines, representing the median across all glaciers, emphasise the systematic difference between the two products, demonstrating that TermPicks achieves both lower overall positional offsets and more consistent performance across glaciers compared to AutoTerm. Together, these results indicate that manual delineations from TermPicks provide a closer and more spatially coherent agreement with the reference dataset, while automated extractions from AutoTerm exhibit larger and more variable deviations.

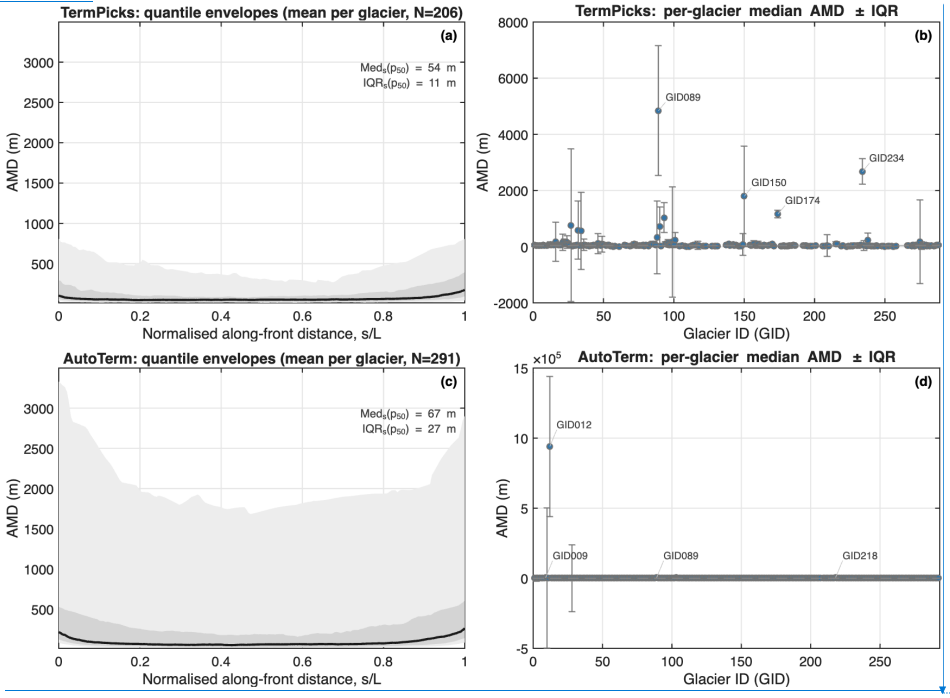

设置了格式: 下标
设置了格式: 默认段落字体
设置了格式: 默认段落字体
设置了格式: 默认段落字体
设置了格式: 默认段落字体
带格式的: 两端对齐

删除了:
In addition, PlanetScope imagery, acquired by a constellation of high-resolution Dove satellites operated by Planet Labs, provides near-daily observations at 3 m spatial resolution. Its fine spatial detail and temporal coverage make it a valuable benchmark for evaluating glacier front delineations. To assess the absolute positional accuracy of our dataset, we selected six representative glaciers across different regions of Greenland—Petermann, Zachariae Isstrøm, Helheim, Kangilinguata, Jakobshavn Isbræ, and Sverdrup glacier (Fig. 1). All selected Planet scenes were cloud-free and acquired on the exact same day of the corresponding image used for digitization. Rather than computing numerical offsets, this comparison focused on visual correspondence between our manually digitized fronts and the clearly identifiable glacier termini in the Planet imagery, with attention to morphological detail such as embayment and lateral margins.
In all six cases, the manually delineated fronts showed strong geometric agreement with Planet imagery, capturing key features with sub-pixel precision relative to the satellite imagery on which the delineations were originally based. Notably, the manual delineations remained reliable even in challenging visual conditions, such as shadowed regions (Fig. 3a) and heavily mélange-affected calving fronts (Fig. 3b–c, f), where frontal morphology remains ambiguous in moderate-resolution imagery. Where available, AutoTerm outputs were also included to show omissions or misalignments in automated results (e.g., missed segments or fragmented fronts), further underscoring the completeness and reliability of our manually derived dataset (Fig. 3a). Furthermore, the inclusion of Kangilinguata Glacier—a region not typically featured in other datasets—and additional comparisons not shown in Fig. 3 underscore the spatial coverage advantage of our dataset. These Planet-based comparisons confirm that our product achieves high absolute positional accuracy and geometric fidelity under diverse glaciological and imaging conditions, providing a robust foundation for the subsequent relative evaluation of large-scale calving front products.

带格式的

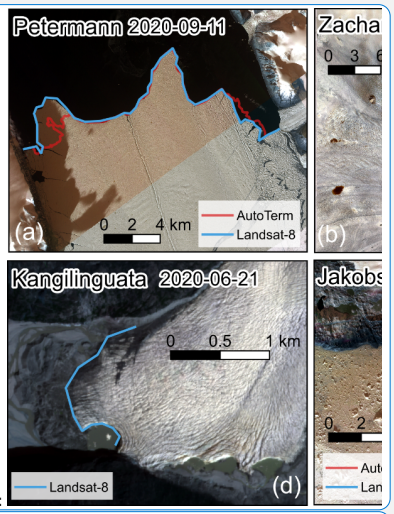

Figure 3: Average minimum distance (AMD) statistics between GrTPD and TermPicks (a–b) and AutoTerm (c–d), using only same-date terminus pairs. (a,c) AMD profiles are evaluated along the normalised along-front coordinate (s/L) and summarized across all included glaciers, showing the median p50(s) (solid line), the interquartile range p25–p75 (dark shading), and the 10–90% range p10–p90 (light shading); the annotation reports Med (p50) and IQR (p50), i.e., the median and interquartile range of the median curve along s. (b,d) Glacier-wise median AMD (points) with within-glacier variability (error bars) plotted against glacier ID (GID); the dashed line indicates the overall median across glaciers, and labelled points highlight the largest-mismatch cases. Distances are computed in a common geographic reference frame; lower AMD indicates closer agreement with the manual delineations.

In addition to the ice sheet-wide statistical comparison, we examine the temporal consistency of glacier terminus positions at the scale of individual outlet glaciers. Specifically, we focus on the glaciers illustrated in Fig. 1 and present detailed spatial overlays and time-series comparisons of terminus positions to evaluate the agreement in temporal evolution among datasets, rather than relying solely on aggregated positional offsets. Kangaasarsuup Sermia glacier, which is not included in any of the existing datasets, was excluded from this comparison. Where overlapping scenes were available, we compared manually delineated fronts in this study with those from each dataset using both visual overlays and distance-based metrics, with the AMD used to quantify spatial offset.

We compared GrTPD presented in this study with several widely used, high-quality calving front products, including the time series compiled by TermPicks (Goliber et al., 2022), MEaSUREs (Black and Joughin, 2023), CALFIN(Cheng et al., 2021a), and AutoTerm (Zhang et al., 2023). Figures 4-8 illustrate case studies for Petermann Gletsjer, Jakobshavn Isbræ, Zachariae Isstrøm, Helheim Gletsjer, and Sverdrup Gletsjer, respectively. For each glacier, we present visual overlays of multi-source ice front positions and corresponding AMD-based offset profiles for three representative dates, along with a long-term time series comparison. Across all sites, the results indicate that manually delineated ice fronts generally show closer agreement and greater positional consistency than automated methods, particularly in visually complex regions. These include mélange-filled fjords, frontal rifting zones, shadowed margins, and lateral embayment, where automated algorithms often fail to preserve morphological detail or misplace the terminus. In earlier years or under challenging image conditions (e.g., mélange or cloud), AutoTerm and CALFIN exhibit large offset(>1km) and reduced morphological precision, often smoothing over frontal curvature or omitting finer-scale features. These deficiencies are especially pronounced in early Landsat scenes and low-contrast fjord settings. For example, at Petermann Gletsjer (Figs. 4a–c), irregular ice front morphology combined with extensive shadowing and mélange cover leads to substantial discrepancies, with automated outputs frequently misaligning with the true ice–ocean boundary. At Jakobshavn Isbræ (Fig. 5a), lateral mélange accumulation obscures the terminus, causing AutoTerm to deviate significantly from other datasets. A particularly notable error occurs in Fig. 5c, where shadowed side regions are misclassified as part of the calving front, resulting in the omission of a retreat signal during a known disintegration phase. For Zachariae Isstrøm (Figs. 6b–c), algorithmic misidentification of surface fractures as the calving margin inflates the spatial offset, particularly in zones where the actual terminus is fragmented or poorly defined. For Helheim (Figs. 7b–c), low image contrast and poorly defined lateral margins lead to deviations exceeding 2 km in the automatically extracted fronts. In contrast, manual delineations capture subtle structures such as ice tongue protrusions and calving embayment concavities with greater fidelity, supporting their use as a reference for both model boundary conditions and algorithm training. These examples highlight common challenges in automated products when faced with ambiguous spectral signals or complex frontal configurations and reinforce the added

删除了:
带格式的: 题注, 两端对齐, 缩进: 首行缩进: 0 字符
删除了: Visual c
设置了格式: 下标
删除了: omparison of this manually delineated calving fro ... [26]
删除了: ↵
删除了: ↵
带格式的: 两端对齐, 缩进: 首行缩进: 2 字符
删除了: To evaluate the consistency of this datasetthe time se ... [27]
删除了: also …ompared GrTPD the dataset ... [28]
带格式的: 两端对齐
设置了格式: 字体: (中文) Times New Roman
设置了格式 ... [29]
删除了: … ADDIN EN.CITE ... [30]
删除了: Due to the scale of our dataset, a glacier-by-glacier ... [31]
设置了格式: 字体: (中文) Times New Roman
设置了格式: 字体: (中文) Times New Roman
删除了: Petermann… ... [32]
删除了: Jakobshavn Isbræ
删除了: Zachariae Isstrøm
删除了: Helheim
设置了格式 ... [33]
设置了格式 ... [34]
设置了格式: 字体: (默认) Times New Roman
删除了: Sverdrup glaciers… respectively. For each glacier, w ... [35]
设置了格式: 字体: (默认) Times New Roman
删除了: Petermann Glacier…(Figs. 4a–c), irregular calving . ... [37]
设置了格式 ... [36]

interpretive value of high-quality manual delineations under challenging observational conditions. The delineations produced in this study remain consistent and structurally accurate even in these environments, highlighting the added value of expert interpretation.

In addition, GrTPD exhibits well consistency with other manually compiled ice front products in capturing both seasonal and interannual glacier dynamics. Time series comparisons with TermPicks Goliber and Black (2021) and MEaSUREs (Black and Joughin, 2023) reveal close alignment across multiple glaciers and observation periods (Figs. 4-8g). For example, at Petermann Gletsjer, the long-term position change trends are highly consistent among the three datasets, confirming their shared capacity to resolve broad-scale frontal evolution (Fig.4g). The time series in Fig.6g and Fig.8g further supports that close correspondence between our dataset and MEaSUREs across the observation period. Notably, the 2004–2005 calving event and the subsequent advance were also captured (Fig. 6g). GrTPD resolves seasonal fluctuations and short-term variability that are consistent with MEaSUREs during overlapping years, while also extending the record back to the early 2000s, providing enhanced temporal continuity for long-term monitoring of Zachariae Isstrøm and Sverdrup Gletsjer. Offset profiles computed using the AMD metric further substantiate this agreement. At Petermann Gletsjer, the AMD between our dataset and the TermPicks or MEaSUREs products is 202.2 m for 2003, 49.3 m for 2017, and 68.6 m for 2020 (Fig. 4d–f). The larger deviation in 2003 reflects the presence of mélange and complex frontal geometry, which challenge all methods. At Jakobshavn Isbræ (Fig. 5d–f), mean offsets range from 68.9 to 135.7 m, with the highest values again associated with earlier imagery and dynamic terminus changes. For Zachariae Isstrøm (Fig. 6d–f), AMD values range from 45.6 to 94.1 m across three dates, with strong spatial alignment observed in clearer scenes such as 2018 (Fig. 6e). For Sverdrup Gletsjer (Figs. 8d–f), the AMD values ranged from 73.8 m to 110.7 m across the three observation dates, showing good overall agreement without significant deviations.

删除了: our dataset
删除了: strong
删除了: calving
删除了:
删除了: ~~(Goliber et al., 2022)~~
删除了: a
设置了格式: 非删除线
删除了: Petermann Glacier,
删除了: Our product
删除了: Isstrom
删除了: glacier
删除了: Average Minimum Distance (
删除了:)
删除了: At Petermann, the AMD between our dataset and TermPicks and MEaSUREs is 202.2 m (2003), 49.3 m (2017), and 68.6 m (2020), respectively …
删除了: Glacier

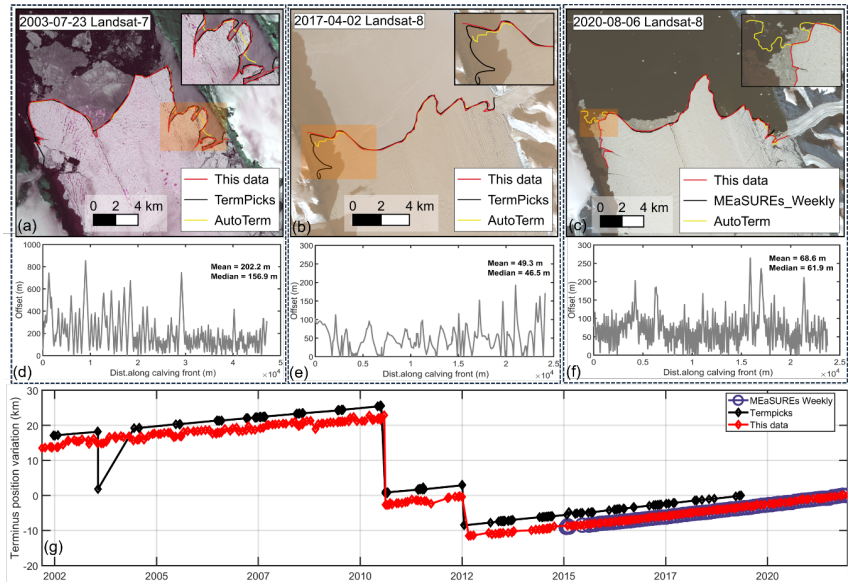

Figure 4: Comparison of delineated calving fronts for Petermann Gletsjer, on three dates (2003-07-23, 2017-04-02 and 2020-08-06). (a–c) overlay this study's fronts (red) with TermPicks (black), AutoTerm (yellow) and MEaSUREs Weekly to Monthly (black) on Landsat scenes; insets zoom in on areas of complex mélange cover or irregular geometry. (d–f) show the along-front offset profiles (AMD) for each date. (d) and (e) show comparisons between this dataset and TermPicks, corresponding to (a) and (b), respectively. (f) compares this dataset with MEaSUREs Weekly, corresponding to (c). Each profile displays both the average and median offsets. (g) presents the time series of manually delineated ice front position variation (km) from 2002 through 2021.

删除了: **Glacier**

删除了: **calving**

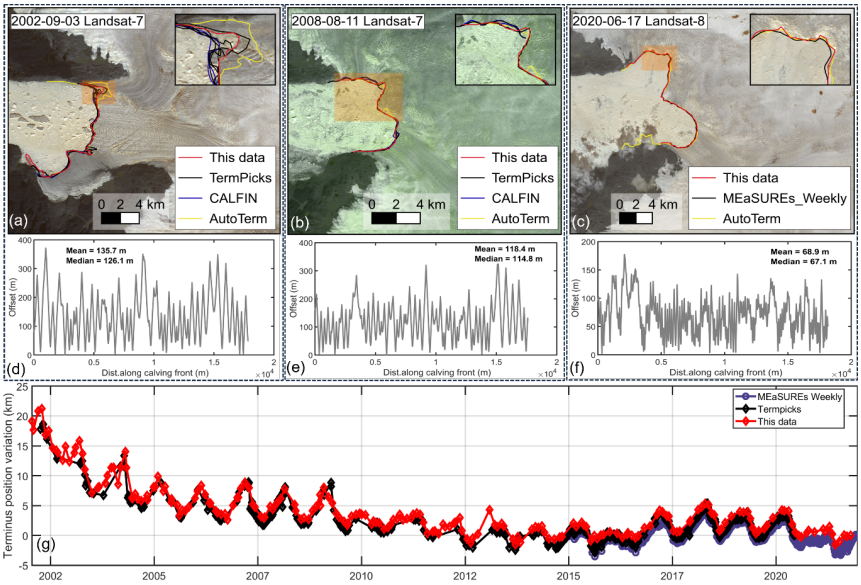

Figure 5: Spatial and quantitative comparison of calving fronts for Jakobshavn Isbræ Glacier at three representative dates (2002-09-03, 2008-08-11, 2020-06-17). (a–c) show this study's delineations (red) alongside TermPicks (black), CALFIN (blue), AutoTerm (yellow) and MEaSUREs Weekly to Monthly (black). Insets highlight zones of mélange or lateral embayment complexity. (d–f) plot the along-front offset distributions. (d) and (e) show comparisons between this dataset and TermPicks, corresponding to (a) and (b), respectively. (f) compares this dataset with MEaSUREs Weekly, corresponding to (c). Each profile displays both the average and median offsets. (g) presents the time series of manually delineated ice front position variation (km) from 2002 through 2021.

删除了: **calving**

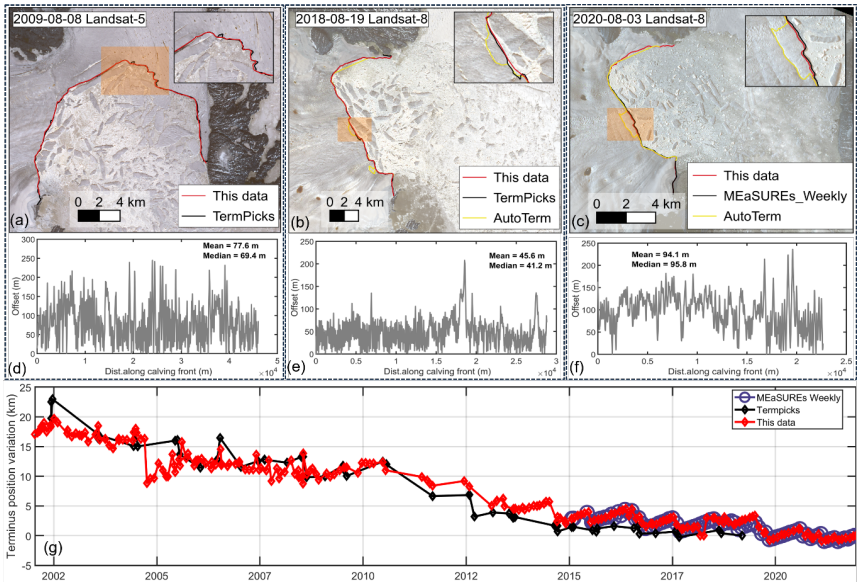

Figure 6: Multi-temporal assessment of Zachariae Isstrøm calving front positions on 2009-08-08, 2018-08-19 and 2020-08-03. (a–c) overlay our manual fronts (red) with TermPicks (black), AutoTerm (yellow) and MEaSUREs Weekly to Monthly (black) on Landsat images; zoomed insets show areas of high morphological complexity. Panels (d–f) illustrate along-front offset profiles for each date. (d) and (e) show comparisons between this dataset and TermPicks, corresponding to (a) and (b), respectively. (f) compares this dataset with MEaSUREs Weekly, corresponding to (c). Each profile displays both the average and median offsets. (g) presents the time series of manually delineated calving front position variation (km) from 2002 through 2021.

删除了: **Isstrom**

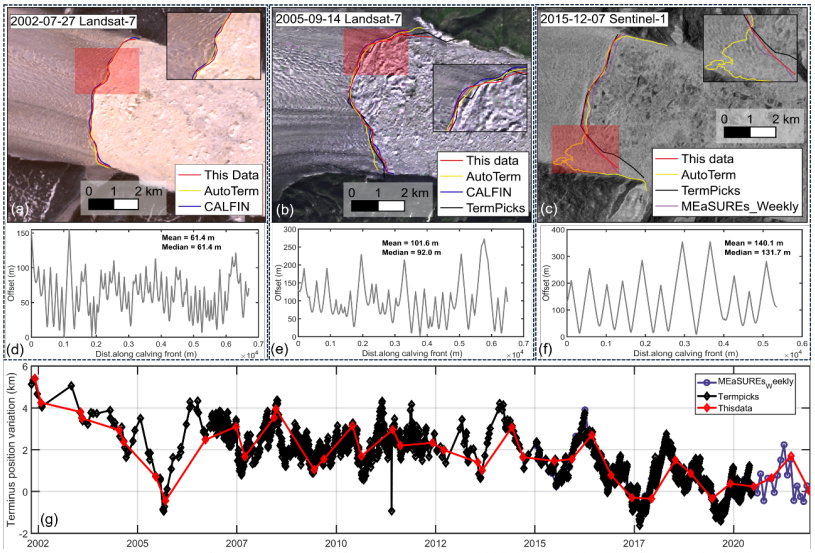

Figure 7: Multi-temporal assessment of Helheim calving front positions on 2002-07-27, 2005-09-14 and 2015-12-07. (a–c) overlay our manual fronts (red) with TermPicks (black), CALFIN (blue), AutoTerm (yellow) and MEaSUREs Weekly to Monthly (purple) on Landsat and Sentinel-1 images; zoomed insets show areas of high morphological complexity. Panels (d–f) illustrate along-front offset profiles for each date. (d) show comparisons between this dataset and CALFIN, corresponding to (a). (e) and (f) compares this dataset with TermPicks, corresponding to (b) and (c), respectively. Each profile displays both the average and median offsets. (g) presents the time series of manually delineated calving front position variation (km) from 2002 through 2021.

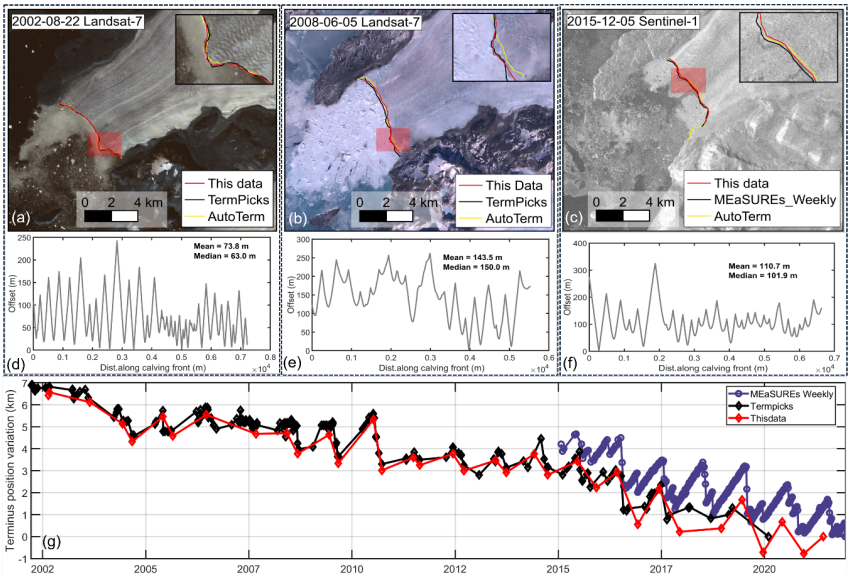

Figure 8: Multi-temporal assessment of Sverdrup Gletsjer calving front positions on 2002-08-22, 2008-06-05 and 2015-12-05. (a–c) overlay our manual fronts (red) with TermPicks (black), AutoTerm (yellow) and MEaSUREs Weekly to Monthly (black) on Landsat and Sentinel-1 images; zoomed insets show areas of high morphological complexity. Panels (d–f) illustrate along-front offset profiles for each date. (d) and (e) show comparisons between this dataset and TermPicks, corresponding to (a) and (b), respectively. (f) compares this dataset with MEaSUREs Weekly, corresponding to (c). Each profile displays both the average and median offsets. (g) presents the time series of manually delineated calving front position variation (km) from 2002 through 2021.

Across all comparative analyses, GrTPD shows good agreement with existing reference products. In comparison with other manually curated datasets, such as TermPicks (Goliber et al., 2022) and MEaSUREs (Black and Joughin, 2023), GrTPD captures comparable seasonal and interannual patterns in glacier terminus variability. It should be noted, however, that the temporally dense sampling illustrated in selected examples does not represent the sampling characteristics of the entire dataset. Seasonal or sub-seasonal coverage is achieved only for a subset of glaciers, depending on satellite data availability and image quality. For some small or less frequently imaged glaciers, temporal sampling is constrained by data gaps, and terminus positions are recorded whenever suitable imagery is available rather than at fixed seasonal intervals. These limitations reflect inherent constraints of satellite coverage and do not detract from the overall consistency and representativeness of the dataset at regional and ice-sheet scales.

3 Data product and usage notes

The dataset described in this study provides manually delineated ice front positions for 465 glaciers across Greenland, spanning the period 2002 to 2021. It includes 19,171 individual terminus delineations

删除了: our manually delineated calving front dataset

删除了: demonstrates

删除了: high positional consistency with

删除了: , with mean offsets typically ranging from 40 to 100 m depending on glacier geometry, image quality, and surface contrast

删除了: While automated and semi-automated methods perform well in clear, high-contrast conditions, our product consistently outperforms them in more challenging environments—such as mélange-filled fjords, shadowed regions, and areas of low contrast—by preserving fine-scale morphological detail, including rifts, lateral embayments, and ice tongue structures that are often misrepresented or omitted by algorithmic approaches (Baumhoer et al., 2019).

带格式的: 两端对齐

删除了: t

删除了: his product captures similar seasonal and interannual trends but offers key advantages in spatial and temporal coverage. ~~Specifically, it provides the longest continuous record to date (2002–2021), near-complete coverage of Greenland's marine-terminating outlet glaciers (~290), and a higher sampling frequency suitable for resolving short-term dynamic events.~~ These strengths are further corroborated by high-precision agreement with PlanetScope imagery, where positional discrepancies are consistently below 10 m, despite the coarser resolution of our primary input data (10–30 m).

删除了: Overall, the validation results establish our dataset as a robust benchmark for glacier front monitoring and time series analysis. It offers not only a reliable foundation for modeling glacier dynamics at high resolution, but also a critical reference standard for training and validating automated calving front detection algorithms—particularly in observationally complex or poorly constrained regions.

删除了: calving

删除了: ~290

删除了: outlet

带格式的: 两端对齐

删除了: approximately 12,000 individual calving front positions

offering broad spatial coverage and seasonal to multi-year temporal resolution (Fig. 9). The full dataset is publicly available at https://doi.org/10.5281/zenodo.18137398 (Xi et al., 2026). For each glacier, the dataset includes a short centerline representing the local ice-flow direction at the terminus, enabling quantification of terminus-position variability and associated dynamic changes. Centerlines were constructed from a robust reference point defined as the median position of all terminus midpoints for a given glacier and were scaled adaptively according to glacier size. Centerline integration followed gridded ice-flow velocity fields (Gardner et al., 2019) with an inertial constraint to suppress small-scale directional noise, while downstream segments lacking reliable velocity information were extended using the dominant upstream centerline orientation.

The dataset is organized in a GeoPackage (GPKG) structure by glacier ID, with all delineations for a given glacier stored within a single layer. Glacier ID follow the naming conventions of the TermPicks (Goliber et al., 2022) and AutoTerm (Zhang et al., 2023) datasets to facilitate cross-dataset comparison and integration. For glaciers not included in AutoTerm, identifiers were assigned sequentially following the same numbering scheme, ensuring internal consistency across the dataset. All spatial data are provided in the WGS 84 geographic coordinate system (EPSG:4326), ensuring compatibility with standard GIS and remote-sensing software. Each terminus is accompanied by structured metadata with the following attributes:

- ID – unique glacier identifier (GID*xxx*)
- GlacierNam – official glacier name
- GlacierTyp – glacier terminus type (MT, LT, LaT, or PG; 2021)
- Date – acquisition date in the format YYYY-MM-DD
- Satellite – platform name (e.g., Landsat-7, Sentinel-2)
- ImagePath – source imagery used for digitization
- Method – digitization tool used (GEEDiT or ArcGIS)
- nvert – number of vertices composing the terminus polyline
- len_km –terminus length (km)

Metadata fields are formatted using a consistent schema across all glacier layers, enabling straightforward filtering, aggregation, and time-series analysis by date, season, satellite sensor, glacier type, and other attributes.

This dataset enables the analysis of glacier terminus variability across a wide range of temporal scales, from multi-year retreat trends to seasonal and sub-seasonal fluctuations. The time series from individual glaciers highlight a diverse range of calving front behaviors, including episodic calving events (Fig. 4), progressive multi-year retreat (Fig. 6, 8), and regular seasonal advance–retreat cycles (Fig. 5, 7). Owing to variability in satellite availability and cloud conditions, temporal sampling density varies among glaciers. For most glaciers, typical sampling intervals range from approximately three to five months (Fig. 9). Glaciers of scientific interest or exhibiting strong frontal variability—such as Jakobshavn Isbræ and Helheim Gletsjer—are represented at substantially higher temporal frequency, supporting detailed analyses of short-term terminus dynamic. Beyond its observational utility, the dataset has also been applied as a time-varying boundary condition in high-resolution transient ice flow modeling, enhancing model-data integration (Lu et al., 2025).

删除了: sub-seasonal
删除了: across nearly two decades
删除了: https://doi.org/10.5281/zenodo.16879054
删除了: .
设置了格式: 字体: (中文) Times New Roman
删除了: The dataset is organized into a GeoPackage structure by glacier ID, with all delineations for a given glacier stored as an individual GeoPackage and named according to the AutoTerm
删除了: convention to facilitate flexible queries, analysis, and integration with existing studies. For glaciers not included in AutoTerm, IDs were assigned based on the names of their nearest neighboring glaciers. For example, a glacier located near GID091 is named ~~*New_NeighborGID091.shp*~~, indicating that it is a newly identified glacier front assigned based on its proximity to GID091. In addition, files named *New_NeighborGID091_x.shp* (where *x* = 1, 2, …) indicate multiple newly digitized calving fronts located near GID091. In total, 69 glaciers in this dataset have calving front positions that are newly recorded compared with those in the AutoTerm dataset. All spatial data are georeferenced in WGS 84 geographic coordinates (EPSG:4326), ensuring compatibility with common GIS and remote sensing tools
设置了格式: 字体: 倾斜
设置了格式: 字体: (默认) Times New Roman, (中文) Times New Roman, 法语
设置了格式: 字体: (默认) Times New Roman, (中文) Times New Roman, 法语
移动了(插入) [2]
移动了(插入) [3]
删除了:
上移了 [3]: <#>Satellite – platform name (e.g., Landsat-7, Sentinel-2)
删除了: <#>Date –acquisition date in the format YYYY-MM-DD Season
删除了: <#>Date –acquisition date in the format YYYY-MM-DD
删除了: <#>classified as 'Melt' (May–September) or 'Non-Melt' (all other months)
删除了:
带格式的: 两端对齐
删除了: To support time series analysis, the metadata are formatted in a consistent structure, allowing users to easily filter or aggregate terminus records by date, season, satellite type, and other relevant attributes. Owing to variability in satellite coverage and cloud conditions, the temporal sampling density differs among glaciers. For most glaciers, typical intervals range from approximately three to five months (Fig. 9), whereas glaciers with higher scientific interest or active frontal variability—such as Jakobshavn Isbræ and Helheim—are captured at higher temporal frequency. ... [38]
删除了: both long-term retreat trends and seasonal calving front dynamics
删除了: Centerline length was scaled by the spatial extent of the terminus observations (90th percentile radius of terminus-ver ... [39]

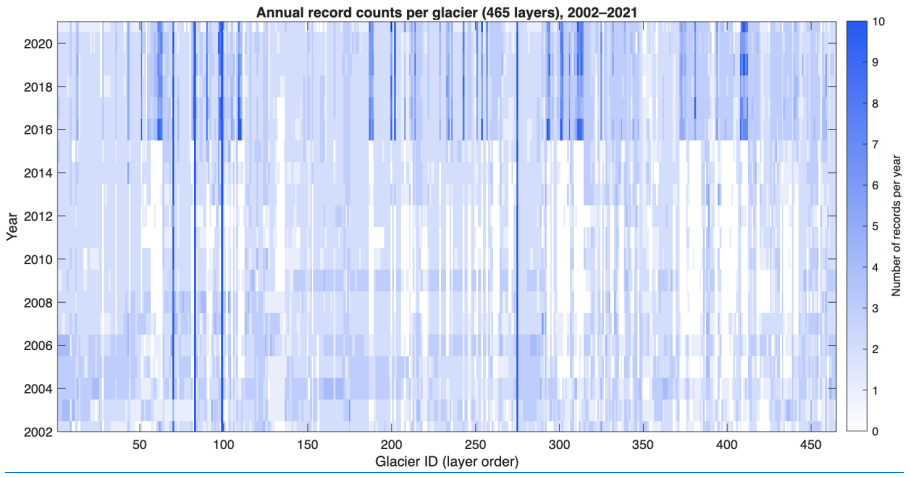

Figure 9: Ice front positions delineation density (2002–2021) for 465 Greenland glaciers. Each column represents a glacier, each row a calendar year, and the colour scale indicates the number of manually digitized ice front positions per glacier per year.

Beyond marine-terminating glaciers, GrTPD extends systematic terminus observations to land-terminating and lake-terminating glaciers that have been largely absent from previous manually delineated datasets. For these glacier types, the combination of consistent terminus delineations and glacier-specific centerlines enables quantitative assessment of frontal migration along a physically meaningful, flow-oriented reference framework. Figure 10 presents example analyses for several lake-terminating glaciers, illustrating distinct retreat behaviors and temporal variability that are not captured by marine-focused datasets. For example, glacier GID449 exhibits a regular seasonal advance–retreat cycle throughout the observational period, superimposed on a cumulative net retreat of approximately 1,200 m since 2002. In contrast, glacier GID397 shows relatively stable terminus positions prior to 2016, followed by rapid retreat in subsequent years. Such contrasting patterns highlight the diverse dynamical responses of lake-terminating glaciers and suggest an increasing sensitivity to surface melt processes and proglacial lake evolution in recent years. These examples underscore the added value of incorporating land- and lake-terminating glaciers into Greenland-wide terminus datasets, complementing existing products that primarily focus on marine-terminating systems.

In addition to its direct observational applications, the dataset provides a high-quality reference for the development, validation, and intercomparison of automated glacier terminus delineation algorithms. As shown in the Validation section, GrTPD can be used in conjunction with existing manually delineated products, such as TermPicks, as independent training and evaluation datasets for automated approaches. This enables robust assessment of algorithm performance, generalization, and uncertainty across a broad range of glacier types and environmental conditions that are not fully represented in existing marine-focused datasets.

带格式的: 题注, 左
设置了格式: 字体: (中文) Times New Roman
带格式的: 两端对齐
设置了格式 ... [40]
删除了: ↵
设置了格式: 字体: (中文) Times New Roman
移动了(插入) [1]
删除了: In addition to supporting high-resolution analyses of seasonal glacier dynamics,Beyond its observational utility, the dataset has also been applied as a time-varying boundary condition in high-resolution transient ice flow modeling, enhancing model-data integration (Lu et al., 2025). this dataset provides a compreh ... [41]
设置了格式 ... [42]

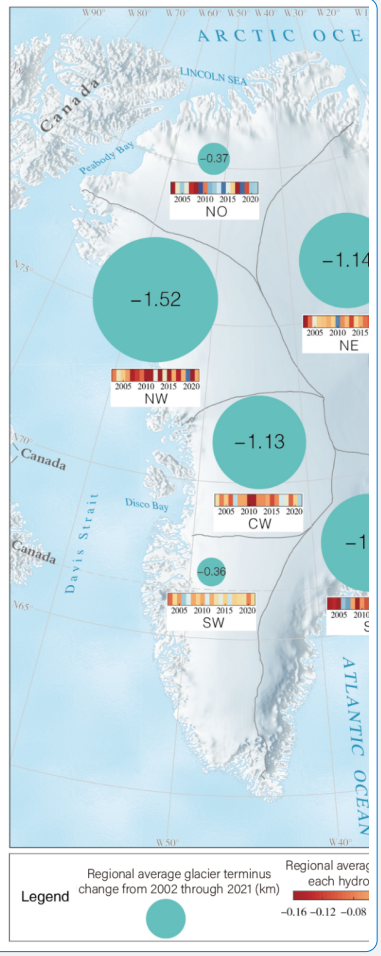

删除了:

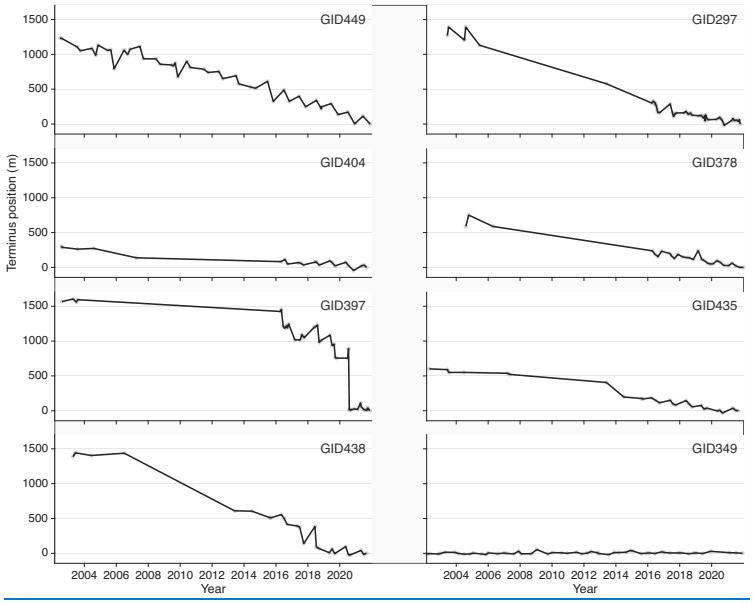

Figure 10: Time series of terminus position change for several lake-terminating glaciers in Greenland derived from the GrTPD dataset. For each glacier, terminus positions are projected along the glacier-specific centerline to quantify frontal migration relative to a fixed upstream reference. Shadow markers indicate individual terminus observations, with temporal sampling varying according to satellite availability.

4 Code and data availability

The complete dataset of manually delineated glacier terminus positions for 465 glaciers across Greenland, covering the period from 2002 to 2021, is publicly available via Zenodo (Xi et al., 2026). All glacier-terminus delineations are provided in GeoPackage (GPKG) format and are organized by glacier identifier, facilitating efficient access and glacier-specific analyses. Terminus delineation was carried out using the open-source Google Earth Engine Digitisation Tool (Lea, 2018) in combination with ArcGIS for supplementary processing and quality control. Supplementary high-resolution reference datasets used for validation and intercomparison (e.g., TermPicks and AutoTerm) are publicly accessible through their respective repositories, subject to the licensing terms and data availability policies of the original data providers. Detailed validation results against TermPicks and AutoTerm are provided in the Supplement.

带格式的: 居中

删除了: **Regional average glacier calving front changes and glacier counts for major Greenland basins, 2002–2021. Each circle on the map is scaled to the net terminus retreat (km) of all marine-terminating glaciers within that basin over the study period; the colour bar beneath each circle shows annual calving front change for each hydrological year. The inset histogram indicates the number of glaciers per basin.**

带格式的: 题注, 两端对齐, 缩进: 首行缩进: 0 字符

删除了: ↵
Figure 11 summarizes the temporal evolution of calving front position by basin, capturing both the magnitude and variability of annual changes. Most basins exhibited consistent retreat over the two-decade period, with pronounced acceleration in frontal retreat occurring in the northeast and southeast since the mid-2000s. In contrast, changes in the southwest and north basins remained relatively limited throughout the record. The interannual dynamics of calving front position change was also basin-dependent. The north, southeast, and northwest basins exhibited the largest year-to-year fluctuations, with 20-year average interannual variability (AVG) values of 0.09 km, 0.12 km, and 0.10 km, and corresponding standard deviations (STD) of 0.11 km, 0.12 km, and 0.08 km, respectively. In contrast, northeast, southwest, and west basins showed more moderate interannual variation (AVG: 0.07 km, 0.04 km, and 0.07 km; STD: 0.07 km, 0.04 km, and 0.07 km, respectively). These results highlight regional heterogeneity in glacier terminus behavior, influenced by both geometric and climatic factors (Grimes et al., 2024; Black and Joughin, 2021), and underscore the value of dense temporal sampling in resolving basin-specific dynamics.

删除了: ~~In addition, the dataset has been successfully integrated as a time-varying boundary condition in high-resolution transient simulations of Sermeq Kujalleq using the Ice-sheet and Sea-level System Model (ISSM) for the period 2016–2022 (Lu et al., 2025).~~ By assimilating sub-monthly calving front positions, the model is able to explain over 76% of the observed ice velocity variations, including seasonal accelerations up to 30 km upstream of the terminus. However, residual spatial and temporal velocity misfits remain, particularly near the grounding line, and are strongly correlated with fluctuations in height above flotation within 10 km of the front. Accounting for these effects through a basal shear stress scaling approach reduces the mean velocity misfit by more than 90%, highlighting the critical role of terminus retreat–induced changes in effective pressure and basal conditions in modulating ice-flow dynamics. These results demonstrate the utility of the dataset not only for frontal change monitoring but also for improving model–data integration and enhancing the physical realism of ice flow pro ... [43]

带格式的: 两端对齐

删除了: The full dataset of manually delineated glacier calving front positions for ~290 outlet glaciers across Greenland from 2002 through 2021 is openly available at https://doi.org/10.5281/zenodo.16879054

删除了: All calving front positions are provided in geopackage format, organized by glacier ID. Comprehensive metadata is included to support filtering by date, sensor platform, and delineation tool. The delineation was performed using the open-source GEEDiT and ArcGIS. Supplementary high-resolution reference data used for validation are accessible via their respective platforms (subject to license or availability).

5 Conclusions

Accurate, spatially extensive records of glacier terminus positions are essential for understanding glacier dynamics, quantifying ice-sheet mass loss, and constraining time-varying boundary conditions in ice-flow models. In this study, we present GrTPD, a new manually delineated dataset of glacier terminus positions for the Greenland Ice Sheet, providing spatially extensive and seasonally targeted coverage across marine-, land-, lake-terminating, and peripheral glaciers. The dataset comprises 19,171 terminus delineations for 465 glaciers spanning the period from 2002 to 2021, derived from multi-source optical and SAR satellite imagery using standardized and reproducible workflows. Systematic validation against existing manually delineated and automated products, including TermPicks and AutoTerm, demonstrates high geometric fidelity and positional consistency of the GrTPD dataset, with median average minimum distances of 54 m relative to TermPicks and 67 m relative to AutoTerm. The comparison further highlights that manual delineations generally exhibit closer agreement and reduced positional variability in visually complex settings, such as regions affected by ice mélange, low contrast, or heterogeneous terminus geometry, where automated approaches remain more sensitive to image quality and surface conditions.

Beyond marine-terminating glaciers, GrTPD extends consistent terminus observations to land-terminating and lake-terminating glaciers that have been underrepresented in previous Greenland-wide manual datasets. The inclusion of glacier-specific centrelines enables flow-oriented analysis of frontal migration across diverse glacier types, revealing contrasting retreat behaviours and temporal variability that complement existing marine-focused records. In addition, the dataset has been applied as a time-varying boundary condition in high-resolution transient ice-flow modelling, demonstrating its utility for model–data integration.

Overall, GrTPD fills critical gaps in the spatial coverage, glacier-type representation, and temporal consistency of existing Greenland terminus datasets. As an independent, manually curated reference product, it provides a robust foundation for studies of glacier dynamics, mass loss, and ice–climate interactions, as well as for the development, validation, and intercomparison of automated glacier terminus delineation algorithms. The dataset is openly available and designed to support future observational, modelling, and machine-learning-based investigations across the Greenland Ice Sheet.

Author Contributions

XL produced, managed, and analyzed the dataset and wrote the manuscript. LJ provided academic supervision and conceptual guidance throughout the study and contributed to the revision and refinement of the manuscript. DL and YL assisted with dataset generation and analysis and supported the data processing workflow. AS and SJL contributed to scientific discussions, provided insights into glaciological processes and data interpretation, and offered critical feedback that improved the manuscript.

删除了: high-resolution records of glacier calving front positions are essential for understanding outlet glacier dynamics, quantifying mass loss, and constraining ice sheet models. This study presents a spatially extensive and seasonally resolved dataset of calving front positions for ~290 outlet glaciers across Greenland between 2002 and 2021. Based on manual delineation from multi-source satellite imagery and supported by standardized workflows, the dataset contains approximately 12,000 calving front positions. Validation against high-resolution PlanetScope imagery and established datasets (TermPicks, AutoTerm, MEaSUREs and CALFIN) shows that the positional accuracy of our manually digitized fronts ranges from ~40 to 100 m, with sub-10 m agreement in some scenes. The dataset demonstrates enhanced performance under challenging conditions—such as mélange cover or complex frontal geometries—where automated algorithms often underperform. In such contexts, human interpretation ensures better fidelity to physical glacier boundaries and preserves fine-scale morphological detail.

带格式的: 两端对齐

删除了: ↵

删除了: Beyond serving as an observational benchmark, the dataset has proven effective in ice-flow modeling applications, where time-varying calving front positions help constrain boundary conditions and improve the realism of transient simulations. Regionally, the dataset reveals substantial spatial heterogeneity in glacier retreat, with stronger multi-year retreat and variability observed in the southeast, northeast, and northwest sectors of the ice sheet.↵ Overall, this contribution provides a high-quality reference for glaciological studies and algorithm development. It fills critical gaps in existing records and is openly available to support future research on calving dynamics, machine learning–based extraction, and model–data integration across the Greenland Ice Sheet.

删除了: study, and

删除了: analysis, and

Competing interests

The contact author has declared that none of the authors has any competing interests.

Acknowledgments

This work was funded by the National Key R&D Program of China (Grant Nos. 2018YFC1406102 and 2017YFA0603103), the Strategic Priority Research Program of the Chinese Academy of Sciences (Grant No. XDA19070104).

References

Andersen, J. K., Fausto, R. S., Hansen, K., Box, J. E., Andersen, S. B., Ahlstrøm, A. P., As, D. v., Citterio, M., Colgan, W. T., Karlsson, N. B., Kjeldsen, K. K., Korsgaard, N. J., Larsen, S. H., Mankoff, K. D., Pedersen, A. Ø., Shields, C. L., Solgaard, A. M., and Vandecrux, B.: Update of annual calving front lines for 47 marine terminating outlet glaciers in Greenland (1999–2018), Geol Surv Den Greenl, doi:10.34194/GEUSB-201943-02-02, 2019.

Baumhoer, C. A., Dietz, A. J., Kneisel, C., and Kuenzer, C.: Automated Extraction of Antarctic Glacier and Ice Shelf Fronts from Sentinel-1 Imagery Using Deep Learning, Remote Sens-Basel, 11, 2529, 2019.

Bevan, S. L., Luckman, A. J., and Murray, T.: Glacier dynamics over the last quarter of a century at Helheim, Kangerdlugssuaq and 14 other major Greenland outlet glaciers, The Cryosphere, 6, 923-937, doi:10.5194/tc-6-923-2012, 2012.

Bjørk, A. A., Kruse, L. M., and Michaelsen, P. B.: Brief communication: Getting Greenland's glaciers right – a new data set of all official Greenlandic glacier names, The Cryosphere, 9, 2215-2218, 10.5194/tc-9-2215-2015, 2015.

Black, T. E. and Joughin, I.: Weekly to monthly terminus variability of Greenland's marine-terminating outlet glaciers, The Cryosphere, 17, 1-13, doi:10.5194/tc-17-1-2023, 2023.

Brough, S., Carr, J. R., Ross, N., and Lea, J. M.: Exceptional Retreat of Kangerlussuaq Glacier, East Greenland, Between 2016 and 2018, Front Earth Sc-Switz, Volume 7 - 2019, 10.3389/feart.2019.00123, 2019.

Brough, S., Carr, J. R., Ross, N., and Lea, J. M.: Ocean-Forcing and Glacier-Specific Factors Drive Differing Glacier Response Across the 69°N Boundary, East Greenland, Journal of Geophysical Research: Earth Surface, 128, e2022JF006857, doi:10.1029/2022JF006857, 2023.

Carr, J. R., Vieli, A., and Stokes, C.: Influence of sea ice decline, atmospheric warming, and glacier width on marine-terminating outlet glacier behavior in northwest Greenland at seasonal to interannual timescales, Journal of Geophysical Research: Earth Surface, 118, 1210-1226, doi:10.1002/jgrf.20088, 2013.

Cassotto, R., Fahnestock, M., Amundson, J. M., Truffer, M., and Joughin, I.: Seasonal and interannual variations in ice melange and its impact on terminus stability, Jakobshavn Isbræ, Greenland, J Glaciol, 61, 76-88, doi:10.3189/2015JoG13J235, 2017.

Catania, G. A., Stearns, L. A., Moon, T. A., Enderlin, E. M., and Jackson, R. H.: Future Evolution of Greenland's Marine-Terminating Outlet Glaciers, Journal of Geophysical Research: Earth Surface, 125, e2018JF004873, doi:10.1029/2018JF004873, 2020.

Catania, G. A., Stearns, L. A., Sutherland, D. A., Fried, M. J., Bartholomaus, T. C., Morlighem, M., Shroyer, E., and Nash, J.: Geometric Controls on Tidewater Glacier Retreat in Central Western Greenland, Journal of Geophysical Research: Earth Surface, 123, 2024-2038, doi:10.1029/2017JF004499, 2018.

Cheng, D., Hayes, W., Larour, E., Mohajerani, Y., Wood, M., Velicogna, I., and Rignot, E.: Calving Front Machine (CALFIN): glacial termini dataset and automated deep learning extraction method for Greenland, 1972-2019, Cryosphere, 15, 1663-1675, 10.5194/tc-15-1663-2021, 2021a.

Cheng, D., Hayes, W., Larour, E., Mohajerani, Y., Wood, M., Velicogna, I., and Rignot, E.: Calving Front Machine (CALFIN): glacial termini dataset and automated deep learning extraction method for Greenland, 1972–2019, The Cryosphere, 15, 1663-1675, doi:10.5194/tc-15-1663-2021, 2021b.
Choi, Y., Morlighem, M., Rignot, E., and Wood, M.: Ice dynamics will remain a primary driver of Greenland ice sheet mass loss over the next century, Commun Earth Environ, 2, 26, doi:10.1038/s43247-021-00092-z, 2021.
Enderlin, E. M., Howat, I. M., Jeong, S., Noh, M. J., Van Angelen, J. H., and Van Den Broeke, M. R.: An improved mass budget for the Greenland ice sheet, Geophys Res Lett, 41, 866-872, doi:10.1002/2013GL059010, 2014.
Fahrner, D., Lea, J. M., Brough, S., Mair, D. W. F., and Abermann, J.: Linear response of the Greenland ice sheet's tidewater glacier terminus positions to climate, J Glaciol, 67, 193-203, doi:10.1017/jog.2021.13, 2021.
Fahrner, D., Slater, D. A., Kc, A., Cenedese, C., Sutherland, D. A., Enderlin, E., de Jong, M. F., Kjeldsen, K. K., Wood, M., Nienow, P., Nowicki, S., and Wagner, T. J. W.: A Frontal Ablation Dataset for 49 Tidewater Glaciers in Greenland, Sci Data, 12, 601, 10.1038/s41597-025-04948-3, 2025.
Fitzpatrick, A. A. W., Hubbard, A., Joughin, I., Quincey, D. J., As, D. V., Mikkelsen, A. P. B., Doyle, S. H., Hasholt, B., and Jones, G. A.: Ice flow dynamics and surface meltwater flux at a land-terminating sector of the Greenland ice sheet, J Glaciol, 59, 687-696, 10.3189/2013JoG12J143, 2013.
Frederikse, T., Landerer, F., Caron, L., Adhikari, S., Parkes, D., Humphrey, V. W., Dangendorf, S., Hogarth, P., Zanna, L., Cheng, L., and Wu, Y.-H.: The causes of sea-level rise since 1900, Nature, 584, 393-397, doi:10.1038/s41586-020-2591-3, 2020.
Fried, M. J., Catania, G. A., Stearns, L. A., Sutherland, D. A., Bartholomaus, T. C., Shroyer, E., and Nash, J.: Reconciling Drivers of Seasonal Terminus Advance and Retreat at 13 Central West Greenland Tidewater Glaciers, Journal of Geophysical Research: Earth Surface, 123, 1590-1607, doi:10.1029/2018jf004628, 2018.
Fürst, J. J., Goelzer, H., and Huybrechts, P.: Ice-dynamic projections of the Greenland ice sheet in response to atmospheric and oceanic warming, The Cryosphere, 9, 1039-1062, doi:10.5194/tc-9-1039-2015, 2015.
Gardner, A. S., Fahnestock, M. A., and Scambos, T. A.: MEaSUREs ITS_LIVE Landsat Image-Pair Glacier and Ice Sheet Surface Velocities (1), Jet Propulsion Laboratory, NASA [dataset], 10.5067/IMR9D3PEI28U, 2019.
Goliber, S., Black, T., Catania, G., Lea, J. M., Olsen, H., Cheng, D., Bevan, S., Bjørk, A., Bunce, C., and Brough, S.: TermPicks: a century of Greenland glacier terminus data for use in scientific and machine learning applications, The Cryosphere, 16, 3215-3233, doi:10.5194/tc-16-3215-2022, 2022.
Greene, C. A., Gardner, A. S., Wood, M., and Cuzzone, J. K.: Ubiquitous acceleration in Greenland Ice Sheet calving from 1985 to 2022, Nature, 625, 523-528, doi:10.1038/s41586-023-06863-2, 2024.
Grimes, M., Carrivick, J. L., and Smith, M. W.: Spatial heterogeneity, terminus environment effects and acceleration in mass loss of glaciers and ice caps across Greenland, Global Planet Change, 239, 104505, https://doi.org/10.1016/j.gloplacha.2024.104505, 2024.
Hall, D. K., Riggs, G. A., Salomonson, V. V., DiGirolamo, N. E., and Bayr, K. J.: MODIS snow-cover products, Remote Sens Environ, 83, 181-194, doi:10.1016/S0034-4257(02)00095-0, 2002.
Holt, E., Nienow, P., and Medina-Lopez, E.: Terminus thinning drives recent acceleration of a Greenlandic lake-terminating outlet glacier, J Glaciol, 70, e9, 10.1017/jog.2024.30, 2024.
Howat, I. M. and Eddy, A.: Multi-decadal retreat of Greenland's marine-terminating glaciers, J Glaciol, 57, 389-396, doi:10.3189/002214311796905631, 2017.
Joughin, I.: MEaSUREs Greenland Image Mosaics from Sentinel-1A and -1B (4), NASA National Snow and Ice Data Center Distributed Active Archive Center [dataset], https://doi.org/10.5067/WXQ366CP8YDE, 2021.
Kc, A., Enderlin, E. M., Fahrner, D., Moon, T., and Carroll, D.: Seasonality in terminus ablation rates for the glaciers in Greenland (Kalaallit Nunaat), The Cryosphere, 19, 3089-3106, 10.5194/tc-19-3089-2025, 2025.
Kehrl, L. M., Joughin, I., Shean, D. E., Floricioiu, D., and Krieger, L.: Seasonal and interannual variabilities in terminus position, glacier velocity, and surface elevation at Helheim and Kangerlussuaq Glaciers from 2008 to 2016, Journal of Geophysical Research: Earth Surface, 122, 1635-1652, doi:10.1002/2016jf004133, 2017.
Lea, J. M.: The Google Earth Engine Digitisation Tool (GEEDiT) and the Margin change Quantification Tool (MaQiT) – simple tools for the rapid mapping and quantification of changing Earth surface margins, Earth Surf. Dynam., 6, 551-561, doi:10.5194/esurf-6-551-2018, 2018.

Loebel, E., Scheinert, M., Horwath, M., Humbert, A., Sohn, J., Heidler, K., Liebezeit, C., and Zhu, X. X.: Calving front monitoring at a subseasonal resolution: a deep learning application for Greenland glaciers, The Cryosphere, 18, 3315-3332, 10.5194/tc-18-3315-2024, 2024.
Lu, X., Sole, A., Livingstone, S. J., Cheng, G., Jiang, L., Chudley, T., Noël, B., and Li, D.: Ice Thickness-Induced Variations in Effective Pressure and Basal Conditions Influence Seasonal and Multi-Annual Ice Velocity at Sermeq Kujalleq (Jakobshavn Isbræ), Geophys Res Lett, 52, e2024GL111092, doi:10.1029/2024GL111092, 2025.
Mohajerani, Y., Wood, M., Velicogna, I., and Rignot, E.: Detection of Glacier Calving Margins with Convolutional Neural Networks: A Case Study, Remote Sens-Basel, 11, 74, 2019.
Moon, T. and Joughin, I.: Changes in ice front position on Greenland's outlet glaciers from 1992 to 2007, Journal of Geophysical Research, 113, doi:10.1029/2007jf000927, 2008.
Moon, T., Joughin, I., and Smith, B.: Seasonal to multiyear variability of glacier surface velocity, terminus position, and sea ice/ice mélange in northwest Greenland, Journal of Geophysical Research: Earth Surface, 120, 818-833, doi:10.1002/2015jf003494, 2015.
Mouginot, J., Rignot, E., Bjork, A. A., van den Broeke, M., Millan, R., Morlighem, M., Noel, B., Scheuchl, B., and Wood, M.: Forty-six years of Greenland Ice Sheet mass balance from 1972 to 2018, Proc Natl Acad Sci U S A, 116, 9239-9244, doi:10.1073/pnas.1904242116, 2019.
Murray, T., Selmes, N., James, T. D., Edwards, S., Martin, I., O'Farrell, T., Aspey, R., Rutt, I., Nettles, M., and Bauge, T.: Dynamics of glacier calving at the ungrounded margin of Helheim Glacier, southeast Greenland, J Geophys Res Earth Surf, 120, 964-982, doi:10.1002/2015JF003531, 2015a.
Murray, T., Scharrer, K., Selmes, N., Booth, A. D., James, T. D., Bevan, S. L., Bradley, J., Cook, S., Llana, L. C., Drocourt, Y., Dyke, L. F. V., Goldsack, A., Hughes, A. L. H., Luckman, A. J., and McGovern, J.: Extensive Retreat of Greenland Tidewater Glaciers, 2000–2010, doi:10.1657/AAAR0014-049,
Nick, F. M., Vieli, A., Andersen, M. L., Joughin, I., Payne, A., Edwards, T. L., Pattyn, F., and van de Wal, R. S. W.: Future sea-level rise from Greenland's main outlet glaciers in a warming climate, Nature, 497, 235-238, doi:10.1038/nature12068, 2013.
Otosaka, I. N., Shepherd, A., Ivins, E. R., Schlegel, N. J., Amory, C., van den Broeke, M. R., Horwath, M., Joughin, I., King, M. D., Krinner, G., Nowicki, S., Payne, A. J., Rignot, E., Scambos, T., Simon, K. M., Smith, B. E., Sørensen, L. S., Velicogna, I., Whitehouse, P. L., A, G., Agosta, C., Ahlstrøm, A. P., Blazquez, A., Colgan, W., Engdahl, M. E., Fettweis, X., Forsberg, R., Gallée, H., Gardner, A., Gilbert, L., Gourmelen, N., Groh, A., Gunter, B. C., Harig, C., Helm, V., Khan, S. A., Kittel, C., Konrad, H., Langen, P. L., Lecavalier, B. S., Liang, C. C., Loomis, B. D., McMillan, M., Melini, D., Mernild, S. H., Mottram, R., Mouginot, J., Nilsson, J., Noël, B., Pattle, M. E., Peltier, W. R., Pie, N., Roca, M., Sasgen, I., Save, H. V., Seo, K. W., Scheuchl, B., Schrama, E. J. O., Schröder, L., Simonsen, S. B., Slater, T., Spada, G., Sutterley, T. C., Vishwakarma, B. D., van Wessem, J. M., Wiese, D., van der Wal, W., and Wouters, B.: Mass balance of the Greenland and Antarctic ice sheets from 1992 to 2020, Earth Syst. Sci. Data, 15, 1597-1616, 10.5194/essd-15-1597-2023, 2023.
Rignot, E. and Kanagaratnam, P.: Changes in the Velocity Structure of the Greenland Ice Sheet, Science, 311, 986-990, doi:10.1126/science.1121381, 2006.
Sakakibara, D. and Sugiyama, S.: Seasonal ice-speed variations in 10 marine-terminating outlet glaciers along the coast of Prudhoe Land, northwestern Greenland, J Glaciol, 66, 25-34, doi:10.1017/jog.2019.81, 2019.
Shepherd, A., Ivins, E., Rignot, E., Smith, B., van den Broeke, M., Velicogna, I., Whitehouse, P., Briggs, K., Joughin, I., Krinner, G., Nowicki, S., Payne, T., Scambos, T., Schlegel, N., Geruo, A., Agosta, C., Ahlstrom, A., Babonis, G., Barletta, V., Blazquez, A., Bonin, J., Csatho, B., Cullather, R., Felikson, D., Fettweis, X., Forsberg, R., Gallee, H., Gardner, A., Gilbert, L., Groh, A., Gunter, B., Hanna, E., Harig, C., Helm, V., Horvath, A., Horwath, M., Khan, S., Kjeldsen, K. K., Konrad, H., Langen, P., Lecavalier, B., Loomis, B., Luthcke, S., McMillan, M., Melini, D., Mernild, S., Mohajerani, Y., Moore, P., Mouginot, J., Moyano, G., Muir, A., Nagler, T., Nield, G., Nilsson, J., Noel, B., Otosaka, I., Pattle, M. E., Peltier, W. R., Pie, N., Rietbroek, R., Rott, H., Sandberg-Sorensen, L., Sasgen, I., Save, H., Scheuchl, B., Schrama, E., Schröder, L., Seo, K. W., Simonsen, S., Slater, T., Spada, G., Sutterley, T., Talpe, M., Tarasov, L., van de Berg, W. J., van der Wal, W., van Wessem, M., Vishwakarma, B. D., Wiese, D., Wouters, B., and Team, I.: Mass balance of the Antarctic Ice Sheet from 1992 to 2017, Nature, 558, 219-+, doi:10.1038/s41586-018-0179-y, 2018.
Sundal, A. V., Shepherd, A., Nienow, P., Hanna, E., Palmer, S., and Huybrechts, P.: Melt-induced speed-up of Greenland ice sheet offset by efficient subglacial drainage, Nature, 469, 521-524, 10.1038/nature09740, 2011.

Tedstone, A. J., Nienow, P. W., Gourmelen, N., Dehecq, A., Goldberg, D., and Hanna, E.: Decadal slowdown of a land-terminating sector of the Greenland Ice Sheet despite warming, Nature, 526, 692-695, 10.1038/nature15722, 2015.
Wood, M., Rignot, E., Fenty, I., An, L., Bjork, A., van den Broeke, M., Cai, C., Kane, E., Menemenlis, D., Millan, R., Morlighem, M., Mouginot, J., Noel, B., Scheuchl, B., Velicogna, I., Willis, J. K., and Zhang, H.: Ocean forcing drives glacier retreat in Greenland, Sci Adv, 7, doi:10.1126/sciadv.aba7282, 2021.
Xi, L., Liming, J., Daan, L., Yi, L., Andrew, S., and Stephen J., L.: Ice front positions for Greenland glaciers (2002–2021): a spatially extensive seasonal record and benchmark dataset for algorithm validation (4.0), Zenodo [dataset], doi:10.5281/zenodo.18137398, 2026.
Zhang, E., Catania, G., and Trugman, D. T.: AutoTerm: an automated pipeline for glacier terminus extraction using machine learning and a "big data" repository of Greenland glacier termini, The Cryosphere, 17, 3485-3503, doi:10.5194/tc-17-3485-2023, 2023.